TOWARDS PRACTICAL APPLICATIONS FOR MOLECULAR LOGIC GATES: "AND" LOGIC AS AN ADDITIONAL LAYER OF SELECTIVITY IN SINGLET OXYGEN RELEASE FOR PHOTODYNAMIC THERAPY

A THESIS SUBMITTED TO
THE GRADUATE SCHOOL OF NATURAL AND APPLIED SCIENCES
OF
MIDDLE EAST TECHNICAL UNIVERSITY

BY

SURİYE ÖZLEM

IN PARTIAL FULFILLMENT OF THE REQUIREMENTS

FOR

THE DEGREE OF MASTER OF SCIENCE

IN

CHEMISTRY

JUNE 2008

Approval of the thesis:

TOWARDS PRACTICAL APPLICATIONS FOR MOLECULAR LOGIC GATES: "AND" LOGIC AS AN ADDITIONAL LAYER OF SELECTIVITY IN SINGLET OXYGEN RELEASE FOR PHOTODYNAMIC THERAPY

submitted by **SURİYE ÖZLEM** in partial fulfillment of the requirements for the degree of **Master of Science in Chemistry Department**, **Middle East Technical University** by,

Prof. Dr. Canan Özgen
Dean, Gradute School of **Natural and Applied Sciences**

_____

.Prof. Dr. Ahmet M. Önal
Head of Department, **Chemistry**

_____

Prof. Dr. Engin U. Akkaya
Supervisor, **Chemistry Dept., METU**

_____

Examining Committee Members:

Prof. Dr. Ahmet M. Önal
Chemistry Dept., METU

_____

Prof. Dr. Engin U. Akkaya
Chemistry Dept., METU

_____

Prof. Dr. Metin Zora
Chemistry Dept., METU

_____

Prof. Dr. Özdemir DOGAN
Chemistry Dept., METU

_____

Dr. Ö. Altan BOZDEMİR
Researcher

_____

Date: _____

I hereby declare that all information in this document has been obtained and presented in accordance with academic rules and ethical conduct. I also declare that, as required by these rules and conduct, I have fully cited and referenced all material and results that are not original to this work.

Name, Last Name : SURİYE ÖZLEM

Signature :

ABSTRACT

TOWARDS PRACTICAL APPLICATIONS FOR MOLECULAR LOGIC GATES: "AND" LOGIC AS AN ADDITIONAL LAYER OF SELECTIVITY IN SINGLET OXYGEN RELEASE FOR PHOTODYNAMIC THERAPY

Özlem, Suriye

M.S., Department of Chemistry
Supervisor: Prof. Dr. Engin Umut Akkaya

June 2008, 54 pages

There have been many examples of individual molecular logic gates and molecular equivalents of more complex digital designs in recent years such as half adder, half subtractor, multiplexer. Neverethless, the unresolved issues of addressability and lack of communication between logic gates remain to be the Achille's heel for molecular logic gates. A few years ago we have demonstrated that appropriately decorated bodipy dyes can be very efficient generators for singlet oxygen, thus act as a satisfactory photodynamic agents. As a bonus, these dyes absorb very strongly at 660 nm which is considered to be within the therapeutic window of mammalian tissue.

So, combining our earlier experience in molecular logic gates and rational design of photodynamic agents, we proposed a photodynamic therapy agent that would release singlet oxygen at a much larger rate when the cancer related cellular parameters are above

a threshold value at the same location. Following the survey of the relevant literature for cancer related parameters, we decided that sodium ion concentration and pH (H^+ concentration) could be very promising targets. In the tumor regions the pH can drop below 6 and the Na^+ concentration is also significantly higher then normal tissues. As a result, in the proposed logic system the chemical inputs could be Na^+ and H^+. The system in fact is an automaton which is to seek higher concentration of both hydrogen and sodium ions, and release the toxic agent (singlet oxygen) only when both concentrations are high. Thus, the proposed logic gate is an AND logic gate, the output of which is singlet oxygen.

Keywords: Photodynamic therapy, singlet oxygen, molecular logic gates, AND logic operation

ÖZ

MOLEKÜLER MANTIK KAPISININ PRATİKTEKİ UYGULAMALARI: "VE" KAPISININ FOTODİNAMİK TERAPİDEKİ SİNGLET OKSİJEN ÜRETİMİ İLE İLİŞKİLENDİRİLMESİ

Özlem, Suriye

Yüksek Lisans, Kimya Bölümü

Tez Yöneticisi: Prof. Dr. Engin Umut Akkaya

Haziran 2008, 54 sayfa

Moleküler mantık kapılarıyla ilgili geçmiş yıllarda yapılan birçok çalışma mevcuttur, bunlara toplama, çıkarma ve multiplekser başta olmak üzere daha da karmaşık tasarımlar eşlik etmektedir. Ancak, bu güne kadar moleküler mantık kapılarının yaptığı işlemin sonucunun herhangi bir işlev yerine getiriyor olmaması bu konunun en büyük eksikliğidir. Birkaç yıl önce yaptığımız çalışmalarda düzgün tasarlanmış olan bodipylerin çok verimli birer singlet oksijen kaynağı olduğunu ve dolayısıylada fotodinamik terapi uygulayabildiğini göstermiş bulunmaktayız. Üstelik bu maddelerin absorpladığı dalga boyu insan vücudunun geçirebildiği 660 nm dir.

Dolayısıyla, moleküler mantık kapıları ve fotodinamik terapiyle ilgili önceden edindiğimiz deneyimlerimizi birleştirerek tasarladığımız fotodinamik terapi ajanı, kanserli bölgedeki bazı madde miktarlarının belli bir değerin üzerinde olduğu zaman, singlet oksijen üretimi en üst seviyede olmaktadır. Yaptığımız araştırmalarda gördük ki;

kanserli dokularda Na^+ iyonu konsantrasyonu ve H^+ (pH düşük) iyonu konsantrasyonu diğer dokulara kıyasla oldukça yüksektir. Bunun sonucu olarak inputları Na^+ ve H^+ ionu olan bir mantık sistemi kurduk. Sistem hem sodyum hem de hidrojen iyonunun yüksek olduğu (kanserli doku) bölgeleri bulup, sadece o bölgelerde aktif olan ve singlet oksijen üretemek suretiyle kanserli hücreyi öldüren küçük bir moleküler makinadır. Dolayısıyla tasarlanan mantık kapısı outputu singlet oksijen olan "VE" mantık kapısıdır.

Anahtar Kelimeler: Fotodinamik terapi, singlet oksijen, moleküler mantık kapıları, ve mantık kapısı uygulamaları

Dedicated to my parents and my brother. . .

ACKNOWLEDGEMENTS

I would like to express my sincere thanks to my supervisor Prof. Dr. Engin U. Akkaya for his guidance, support, endless imagination and patience.

I would like to express my gratitude to the NMR technician Fatoş Doğanel Polat and Seda Karayılan for NMR spectra, excellent friendship and for their patience.

My special thanks go to my mother and father, especially to my brother Taner for their continuous support, patience, encouragement and endless love.

I want to thank Ali Coşkun, Altan O. Bozdemir, Deniz Yılmaz for their guidance and valuable friendship. I also would like to thank our group members Yusuf, Serdar, İlker, Bora, Tuğba, Onur and rest of the SCL members and Gençay for his giving positive energy.

.

TABLE OF CONTENTS

LIST OF TABLES

TABLES

LIST OF FIGURES

FIGURE

LIST OF ABBREVIATIONS

BODIPY	Borondipyrromethene
PDT	Photodynamic therapy
PS	Photosensitizer
NIR	Near infrared
ROS	Reactive oxygen species
ISC	Inter system crossing
PET	Photoinduced electron transfer
LED	Light-emitting diode
PDI	Perylenediimide dye
TFA	Trifluoroacetic acid

CHAPTERS

1. INTRODUCTION

1.1 History of Photodynamic Therapy

Photodynamic therapy (PDT) is an emerging treatment modality for a range of disease classes, both cancerous and noncancerous [1]. It is a modality for the treatment of a variety of oncological, cardiovascular, dermatological, and ophthalmic diseases [2]. The utility of light as a therapeutic agent can be traced back over thousands of years when it was used in Ancient Egypt, India and China to treat a variety of skin diseases like psoriasis, vitiligo, rickets, cancer and psychosis. Whole body sun exposure (heliotherapy) was considered important for the restoration of health in ancient Greece. Sunlight was used in France during 18th and 19th centuries for treating various diseases like tuberculosis, rickets, scurvy, rheumatism, paralysis, edema and muscle weakness. Danish physician Niels Finsen successfully treated small pox using red light and went ahead with the development of carbon arc phototherapy which made use of ultaviolet light for the treatment of cutaneous tuberculosis for which he was awarded Nobel Prize in 1903.

Administration of a photosensitizing agent followed by the irradiation of light on tissues in which the agent is localized was another form of therapy. 3000 years ago vitiligo was treated in India by employing psolarens and light while, Egyptians used different psolarens in 12th century for the treatment of leucoderma [3]. In 1970, ultraviolet A light (PUVA therapy) were used for the treatment of psoriasis and in immunotherapy [4]. Thus it can either be by its direct action on tissue or indirectly by the activation of a photosensitizer which in turn will bring about the therapeutic effect.

Inducing cytotoxicity by the interaction of light and chemical was first reported by Oscar Raab, a medical student working with Professor Herman von Tappeiner, in 1900 while studying the effects of acridine on paramacium Infusoria **.** His pioneering work led to the conclusion that such fluorescent dyes will have future medicinal applications. In 1903, Tappeiner along with dermatologist Jesionek used eosin and sunlight to treat skin tumors . In 1907, Tappeiner together with Jodlbauer demonstrated the requirement of oxygen in photosensitizing reactions and coined the term "*photodynamic action*" to describe the phenomenon [3, 5].

1.2 What is Photodynamic Therapy?

Photodynamic therapy is based on the concept that light-sensitive species or photosensitizers (PSs) can be preferentially localized in tumor tissues upon systemic administration. When such photosensitizers are irradiated with an appropriate wavelength of visible or near infrared (NIR) light, the excited molecules can transfer their energy to molecular oxygen in the surroundings, which is normally in its triplet ground state. This results in the formation of reactive oxygen species (ROSs), such as singlet oxygen ($^1O_2$) or free radicals. ROSs are responsible for oxidizing various cellular compartments including plasma, mitochondria, lysosomal, and nuclear membranes, etc., resulting in irreversible damage of tumor cells. Therefore, under appropriate conditions, photodynamic therapy offers the advantage of an effective and selective method of destroying diseased tissues without damaging adjacent healthy ones [2].

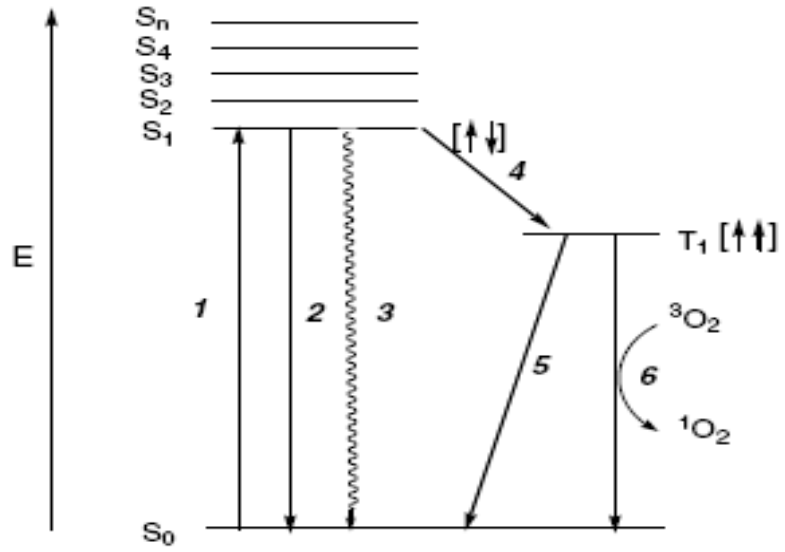

Figure 1. Modified Jablonski diagram. Photophysical processes: 1, absorption; 2, fluorescence; 3, internal conversion; 4, intersystem crossing; 5, phosphorescence; and 6, formation of singlet oxygen $^1O_2$ by energy transfer from T_1 photosensitizer to triplet oxygen $^3O_2$.

The photochemical and photophysical principles of PDT have been extensively studied and are schematically represented in a modified Jablonski diagram shown in Figure 1. Upon illumination, sensitizer molecule gets excited from its ground singlet state (S_0) to short-lived (~10^{-6} seconds) electronically excited singlet state (S_1), which can undergo radiative (fluorescence shown as route 2) and nonradiative (internal conversion indicated as route 3) decay to come back to the ground state (S_0). A good photosensitizer will at this stage undergo a spin forbidden inter system crossing (ISC) (shown as route 4) which requires a spin inversion, converting the photosensitizer to a triplet state (T_1, 10^{-2} seconds) with high efficiency [4]. This transition is spin-forbidden, but a good photosensitizer has nevertheless a high triplet-state yield. The T_1-state is sufficiently long-lived to take part in chemical reactions, and therefore the photodynamic action is mostly mediated by the T_1-state [6]. Triplet state relaxes back to ground state *via* spin forbidden radiative pathway (phosphorescence shown as route 5 in Fig. 1) which imposes relatively long life time for triplet state or by internal conversion (radiationless transitions during collisions with other molecules). In oxygenated environments it undergoes

photochemical process (shown as route 6) which involves an energy transfer between excited triplet state of photosensitizer and stable triplet oxygen ($^3O_2$) producing short lived and highly reactive excited singlet oxygen ($^1O_2$).

Singlet oxygen is actually a highly polarized zwitterion and is considered to be a proficient cytotoxic agent. The short lifetime of singlet oxygen (100-250 ns) limits the diffussion range to approximately 45 nm in cellular medium and hence cannot diffuse more than a single cell length (diameter of human cell ranges from 10-100 μm). Hence, the primary generation of $^1O_2$ warrants for the subcellular structures that can be accessed and destroyed [3].

1.2.1 Cells, Tissues, and Light

Light upon interaction with a tissue surface can be reflected, scattered, transmitted, or absorbed (Figure 2) depending on optical features of the tissue and on the light properties (absorption coefficient, photon energy, power density, exposition time, etc.). The presence of water and highly absorbing endogenous dyes such as melanin and hemoglobin strongly influences light penetration depth into the tissue. Therefore, light penetration depth is highly dependent on the tissue type; however, in the case of most tissues light of the spectral range 600-700 nm penetrates 50-200% deeper than light of the range 400-500 nm. The maximum of skin permeability occurs in the range of 620-850 nm; thus, light of this spectral range (so-called "phototherapeutic window") is predominantly used in phototherapy [7].

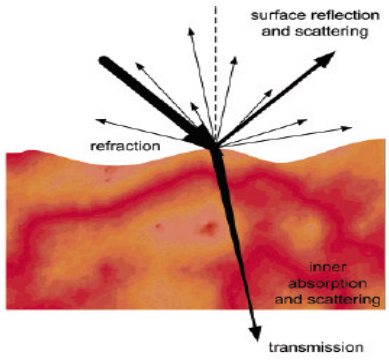

Figure 2. Light interactions with a tissue

Photodynamic therapy (PDT) takes advantage of the interaction between light and a photosensitizing agent to initiate apoptosis of cancer cells [8]. In PDT, instead of directly reacting with cells and tissues the photosensitizing agent becomes activated by light. It does that by transfering its triplet state energy to nearby oxygen molecules to form reactive singlet oxygen ($^1O_2$) species, which cause cytotoxic reactions in the cells [9].

1.2.2 Vital Requirements for an Ideal Photosensitizer

The choice of a photosensitizer and its subsequent phototherapeutic effect depends on its physicochemical properties in the ground and excited states, pharmacokinetic and pharmacodynamic behavior, and photoactivity in vivo [10,11].

Some of the properties essential for an ideal photosensitizer are listed below :

i) It should be chemically pure and of known specific composition with a reproducible synthesis.

ii) It should have high quantum yield for singlet oxygen production for effective destruction of tumor cells.

iii) It should have strong absorption with high extinction coefficient ε at longer wavelength (red) region preferably between 700-800 nm where scattering of light is minimum and tissue penetration is maximum and is sufficiently energetic enough to produce singlet oxygen.

iv) It should have excellent photochemical reactivity, with high triplet state yields (ϕ_f) and long triplet state life times (τ_1) and be able to effectively produce $^1O_2$ and other reactive species. When the triplet energy of sensitizer is lower than 94 kJ/mol (1270 nm), it cannot transfer its energy effectively from triplet state of sensitizer to the ground state triplet oxygen and hence could not produce singlet oxygen.

v) It should possess minimal dark toxicity and only be cytotoxic in presence of light.

vi) It should have preferential retention by target tissue (tumor cells).

vii) It should be rapidly excreted from the body, thus inducing a low systemic toxicity.

viii) Finally it should be synthesizable from easily available precursors and should be stable and easy to dissolve in the body's tissue fluids [3].

ix) Preferably, the photosensitizer should not strongly absorb light of the region 400–600 nm, so that the risk of generalized photosensitivity caused by sunlight would be as small as possible [6].

There is no sensitizer that can be named as ideal for every possible application, but efforts are on in search of perfection and a host of second generation photosensitizers are reported which has set right some of the drawbacks of first generation sensitizers [3].

1.3 Types of photosensitizers

A photosensitizer is a molecule that is activated to an excited singlet state when it absorbs a photon of an appropriate wavelength; it can react with biological targets [12]. Since the first demonstration of the photodynamic action in 1900, great effort has been devoted towards the development of photodynamic therapy agents, which have specific light absorption and tissue distribution properties [13].

1.3.1 First-generation photosensitizers: hematoporphyrin and its derivatives

A first-generation photosensitizer that has been accepted for clinical use is the hematophorphyrin (HpD) derivative, Photofrin, **1** [13]. The first-generation photosensitizers are based on chemically modified natural hematoporphyrin [11,14]. They possess certain limitations such as weak absorption in the phototherapeutic window as well as a relatively poor specificity of uptake and retention with respect to malignant and healthy tissues. In addition, they cause prolonged skin photosensitivity (usually 2-3 months) [15]. In view of the shortcomings encountered by the first generation photosensitizers, researchers around the world are in search of more powerful, efficient and maximum penetrating red light absorbing photosensitizers that can ensure effective treatment for deep lying tumors with minimal side effects.

Photofrin has been accepted for treating various forms of cancer in many countries such as early and late stage lung cancer, superficial and advanced oesophagal cancer, bladder cancer, superficial and early stage gastric cancers, early stage cervical cancer and cervical dysplasia [16]. Eventhough it fulfills certain criterion for ideal

photosensitizers, it suffers from several drawbacks. Its maximum absorption band falls at 630 nm well below the wavelength suggested for maximum tissue penetration and treatment of deep-seated tumors, and its prolonged cutaneous photosensitivity, makes it less attractive for clinical use. Systemic occurrence of porphyrins in the body causes a phototoxic reaction on areas exposed to light. In its mild form, the photosensitivity syndrome is evident as edema, erythema, and lesions on the skin, but in its severe form it can be lethal [6].

Nevertheless, Photofrin had such a lot of success that inspite of these disadvantages it has led to the intense activity in the development of new and improved drugs. In Russia for example derivatized Photofrin, Photoheme is produced and has been accepted and put into clinical use by the Pharmacological Committee of Russia for skin, breast, lung, larynx, gastrointestinal and pharingeal cancers [17]. HpD and its purified derivatives Photofrin, Photosan (developed by Seehof) and Photoheme constitute first generation photosensitizers.

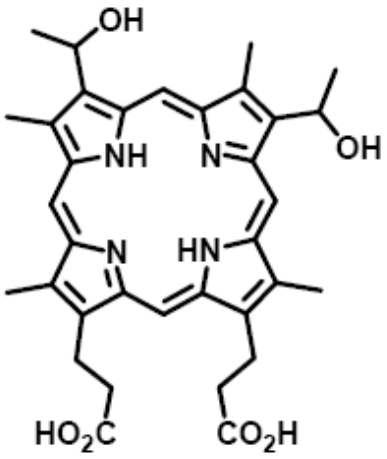

1

Figure 3. Structure of hematophorphyrin, **1**.

1.3.2 Second generation photosensitizers (non-porphyrin photosensitizers)

Due to the certain limitations that the first generation photosensitizers possess, subsequent extensive research helped to develop modern photosensitizers of the second

and third generations. The second generation PDT sensitizers are mainly based on engineered, synthetic, and semisynthetic porphyrins with various substituents at at the pyrrole rings and the methylene bridges. They are structurally homogeneous compounds with long-wavelength absorption bands of high intensity [7]. Second generation photosensitizers are chemically pure, absorb light around 650 nm or longer and induce significantly less skin photosensitivity [18].

The second generation photosensitizers used in clinical trials belong to the groups of porphyrins, phthalocyanines, texaphyrins, chlorins, or bacteriochlorins. These compounds have certain characteristics that make them especially suitable for PDT. An important characteristic is their good ability to generate $^1O_2$ [19].

1.3.2.1 Meso-substituted Porphyrin

The absorption of red light by porphyrins can be strengthened and moved to longer wavelengths with suitable substituents. 5,10,15,20-Tetra(3-hydroxyphenyl)porphyrin (m-THPP), **2**, (Fig. 4) and 5,10,15,20-tetra(4-sulfonatophenyl)porphyrin (p-TPPS4), **3**, (Fig. 4) are substituted porphyrins developed as potential new photosensitizers for PDT. m-THPP is 25–30 times as effective as HpD or Photofrin as a photosensitizer [3].

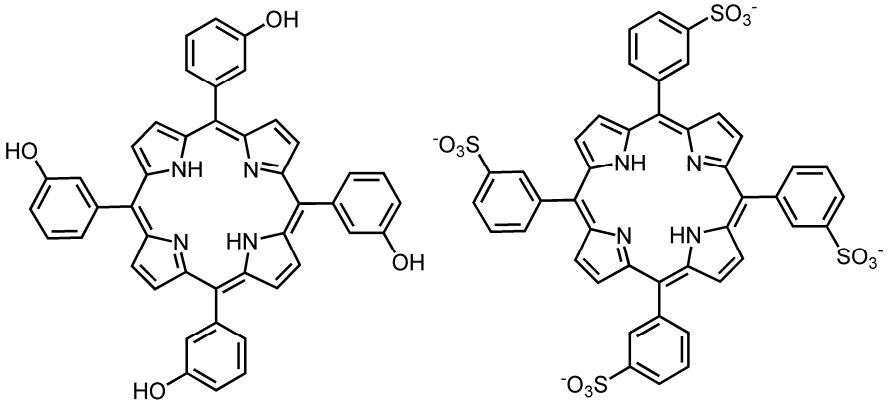

2
5,10,15,20 Tetra(3-hydoxyphenyl)-porphyrin, m-THPP

3
5,10,15,20 Tetra(4-sulfonatophenyl)-porphyrin, p-$TPPS_4$

Figure 4. Meso-substituted porphyrins that have been developed as potential photosensitizers for PDT.

The expansion of the macrocyclic p-system of porphyrins moves their absorption to longer wavelengths and strengthens it [6].

1.3.2.2 Phthalocyanines and naphthalocyanines

The joining of four benzene or naphthalene rings to the b-pyrrolic positions of porphyrins and substituting the methine-bridge carbons with nitrogens, produces phthalocyanines and naphthalocyanines (Fig. 5). Phthalocyanines, absorb very strongly in the red region of the spectrum with absorption maxima at 700 nm and naphthalocyanines at 780 nm [20]. Because these compounds absorb long-wavelength light strongly, they can be used in small doses, such as 0.2–0.5 mg kg^{-1} [21]. In comparison, approximately 1–5 mg kg^{-1} of Photofrin is needed for PDT. Furthermore, as phthalocyanines and naphthalocyanines do not strongly absorb light with in the range of 400–600 nm, the risk of generalized photosensitivity due to sunlight is much smaller than that with porphyrins. The kinetics of phthalocyanines in the body is much faster than that of HpD. Their enrichment factor in tumor is at maximum 1–3 h after injection [6].

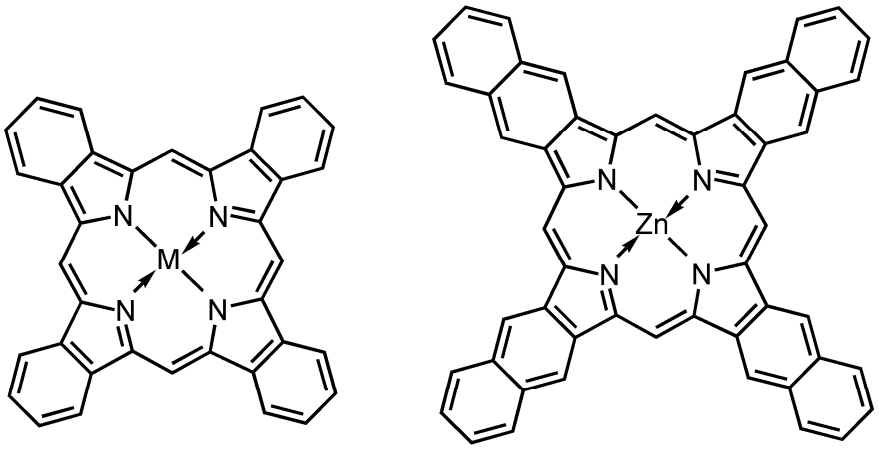

4 M=Zn(II), Phthalocyaninato-Zn(II)
5 M=Cu(II), Phthalocyaninato-Cu(II)

6 Napthalocyaninato

Figure 5. Phthalocyanine and naphthalocyanine derivatives that are relevant to PDT

1.3.2.3 Synthetic Chlorins and Bacteriochlorins

The reduction of a peripheral double bond of a porphyrin strengthens the longest-wavelength absorption band and moves the maximum absorption further to the red up to 680 nm. The dihydroporphyrins thus obtained are called chlorins. In bacteriochlorins, two double bonds on the opposite sides of the macrocycle are reduced, which strengthens and moves their absorption even further to the red to 780 nm [19]. The synthetic chlorine 5,10,15,20-tetra(3-hydroxyphenyl)-2,3- dihydroporphyrin, **7**, (mTHPC), is perhaps the most useful photosensitizer of the synthetic chlorins. mTHPC (Foscan, Biolitec Pharma, Scotland, U.K.), figure 6, has been approved in Europe for use against head and neck cancer, and additional indications have been filed for prostate and pancreatic tumors [22].

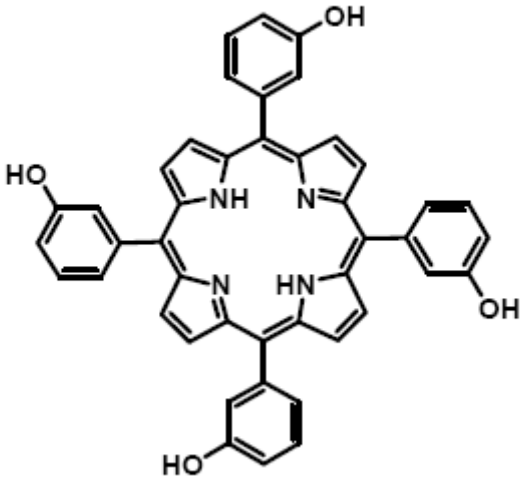

7, mTHPC

Figure 6. Structure of 5, 10, 15, 20-tetra (3-hydroxyphenyl)-2,3- dihydroporphyrin, **7**, (mTHPC)

m-THPP and m-THPC differ only in the reduction degree of the tetrapyrrole ring. The reduced form of m-THPC is more active than m-THPP in PDT [6].

1.3.2.4 Texaphyrins

Texaphyrins are modified porphyrins, in which a phenyl ring replaces one pyrrole ring (Fig. 7). Vogel et al. synthesized porphycene in 1986 for the first time by the McMurry-rearrangement of bipyrrole dialdehydes. Although the yield of the synthesis is low and the starting materials are not readily available, clinical trials on substituted porphycenes are already in progress. Also texaphyrins generate $^1O_2$ efficiently. They can easily be complexed with large metal cations, such as Ln(III) or Lu(III), to give metal complexes that are photoactive in vivo. The Lu(III)-complex of a texaphyrin (LuTex) is a very stable hydrophilic photosensitizer, enriched in tumors very selectively [6].

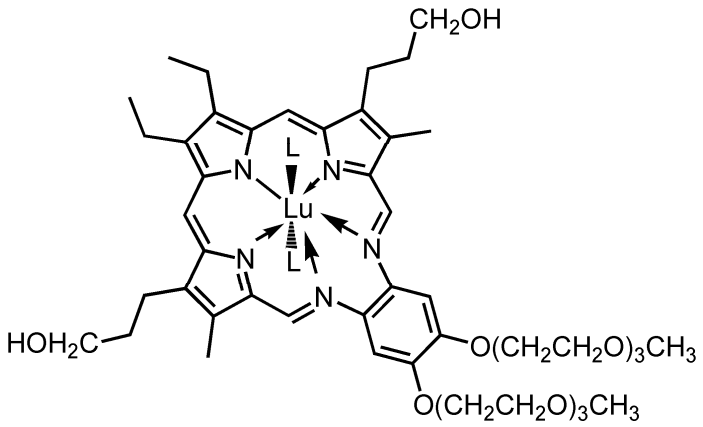

8

Figure 7. Texaphyrinato-Lu(III), a very stable hydrophilic photosensitizer.

These complexes have a strong absorption band in the 600- 900 nm regions, the position of which can be varied by suitable cohice of substituent [23].

1.3.2.5 BF_2 chelated Azadipyromethene dyes

These dyes are studied by O'Shea et al. He has reported the synthesis, photo physical properties and in vitro cellular uptake evaluation of a totally new class of PDT agent of azadipyromethene dyes. A study of the spectroscopic properties of **9** and **10** in chloroform demonstrated that they have a sharp absorption band at 650 nm [24].

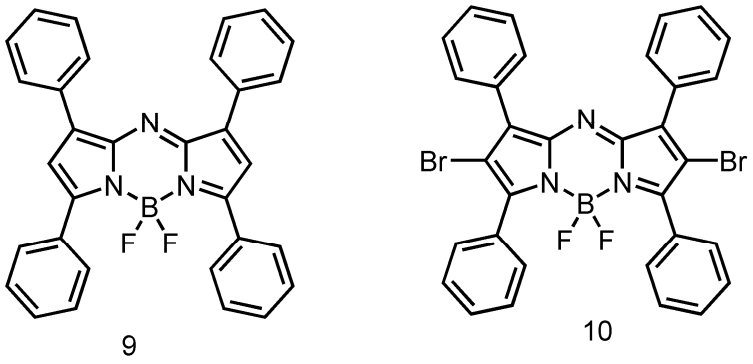

Figure 8. Structures of azadipyromethene dyes

Another example about azadipyromethene dyes synthesized by O'Shea et al. is **11**. In this study, the hypotheses to be tested were whether (i) singlet oxygen generation could be controlled by solution pH and (ii) cells could activate the photosensitizer and as a consequence cause their own death. The ability of **11a**-**d** to modulate singlet oxygen generation in response to an acidic environmental stimulus was tested by trapping with 1,3-diphenylisobenzofuran (DPBF). Photosensitizer **11a**, which does not contain an amine receptor group, showed no significant variance in singlet oxygen generation when analyzed in DMF or DMF with an aliquot of 0.05 M HCl. In comparison, singlet oxygen generation by **11b, c** and **d** displayed a marked reliance upon the presence or absence of a proton source. This would substantiate a PET mechanism being the predominate mode of singlet oxygen control.

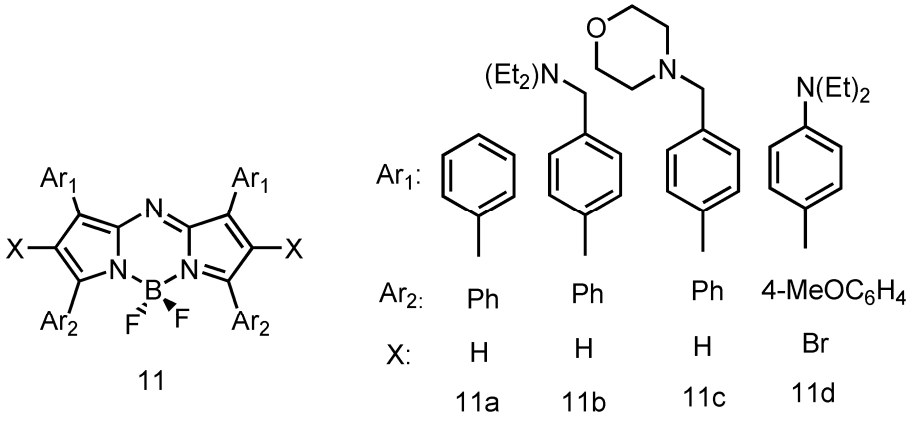

Figure 9. BF_2-chelated azadipyrromethenes.

With this study, they have outlined a new strategy to therapeutic selectivity in which a supramolecular therapeutic agent could manufacture a cytotoxic agent (singlet oxygen) in response to one exogenous stimulus (light) and one endogenous stimulus (microenvironment pH). The absence of the specific endogenous stimulus would switch off the therapeutic function of the photosensitizer thereby providing selectivity [25].

1.3.2.6 Borondipyrromethene (BODIPY) dyes

Nagano et al. report a novel photosensitizer, by focusing on the boron dipyrromethene (BODIPY) fluorophore since BODIPYs generally have high extinction coefficients (ε) and high quantum efficiencies of fluorescence (Φ), which are relatively insensitive to environment [26] (i.e., solvent polarity or pH), and they are also resistant to PDT [27]. Thus, they hypothesized that the BODIPY fluorophore can be transformed into a general photosensitizing chromophore without loss of its unique characteristics. A novel photosensitizer, 2I-BDP, **12**, was developed without loss of the unique characteristics of the BODIPY fluorophore by Nagano et al. They have already shown that BODIPY can be easily modified chemically for the preparation of various derivatives [28].

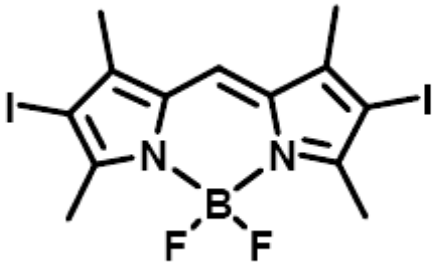

12

Figure 10. Structure of 2I-boron dipyrromethene

A well modified example of a BODIPY derivative, **13**, designed for PDT was introduced to literature by Akkaya and his co-workers. They have demonstrated that novel distyrylboradiazaindacene dyes with bromo substituents on the fluorochrome *p*-system are very efficient singlet oxygen generators.

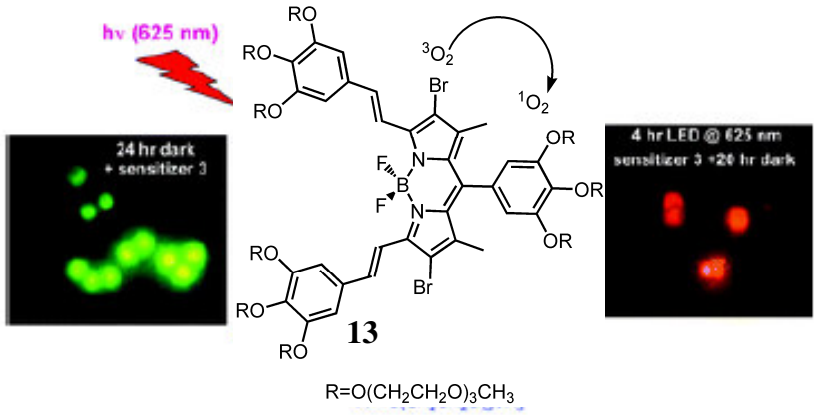

Figure 11. An example of a BODIPY dye designed for PDT.

In addition, these water soluble photosensitizers were shown to have spectacular photoinduced cytotoxicity at very low concentrations and even under low fluence rate LED irradiation. Dark toxicity was nil at the concentration range studied [29].

1.3.2.7 Perylenediimide (PDIs) dyes

PDIs are reddish dyes with very high quantum yields. As such they are not long wavelength dyes. But, by single or double amine substitution on the perylene core, the absorption maxima at these dyes can be shifted up to 750 nm with further appropriate modifications; solubility can be improved [30].

Akkaya et al. have synthesized a series of water-soluble green perylenediimide (PDI) dyes. On red light excitation, these dyes were shown to be efficient generators of singlet oxygen, and in cell culture media, they were shown to display significant light-induced cytotoxic effects on the human erythroleukemia cell line (K-562) [31].

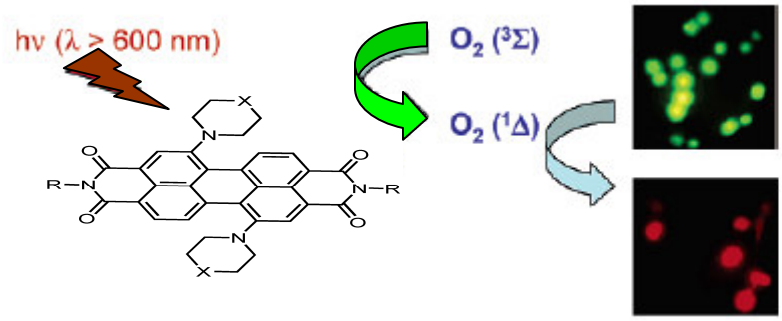

1; R= -CH_2COOH
X= O
2; R= -CH_2COOH
X= N-CH_2CH_2OH
3; R= -$CH(CH_2COH)COOH$
X= O

14

Figure 12. Water-soluble green perylenediimide (PDI) dyes.

1.3.3 Third generation photosensitizers

The third-generation photosensitizers consist of the photosensitizer moiety linked to biomolecules such as polypeptide chains, monoclonal antibodies, proteins, etc., which allow their selective delivery. This strategy overcomes difficulties in molecule recognition and specific binding to the tumor [7].

1.4 Light Sources

The radiation used in PDT is light of the visible and near-infrared regions. The wavelength of light required is dependent on the photosensitizer used. The longest possible wavelength is chosen to reach a therapeutic effect as deep as possible [32]. The light dose required to achieve a certain therapeutic effect is dependent on the photosensitizer used and on the optical properties of the tissue. In Photofrin PDT, the required light dose is normally 50–500 J cm^{-2}, but when second-generation sensitizers with stronger light absorption are used, 10 J cm^{-2} may suffice. To avoid excess heating, the irradiation power should not exceed 200 mW cm^{-2} [6].

1.4.1. Arc lamps

The mercury arc lamp is the workhorse of organic photochemistry, and has some applications in photomedicine. There are three main types. The low-pressure mercury arc operates at room temperature and about 10^{-3} mm pressure: the main emission is a single line at 253.7 nm. Medium-pressure mercury lamps operate at about 1 atmosphere: the emission contains a number of lines, of which 366 nm and 546 nm are the principal ones. The 366 nm line is commonly used to observe the red fluorescence of porphyrins and other dye stuffs. The high-pressure mercury arc operates at ~100 atmospheres and is an intense source: the emission is practically a continuum.

1.4.2 Incandescent lamps

Incandescent lamps are inexpensive and have been used in PDT. For example, in the treatment of basal cell carcinoma using δ-aminolaevulinic acid as a pro-drug, Kennedy and Pettier employed a projector lamp as the light source. Infrared and ultraviolet light are filtered out with filters and a dichroic reflector to give illumination in the required 400-550 nm region (λmax 450 nm).

1.4.3 Light-emitting diodes (LEDs)

They are semiconductor based devices driven by an electric current. The emission is not coherent (this is not a laser source), and is low power, so not much heat is produced. Wavelength can be adjusted by changing the semiconductor, and the devices are small, but they can be bunched together to fit a particular structure. They are finding increasing application. Thus, the LED system recently announced by Diomed consists of a close-packed array of LEDs in a water-cooled head which is designed to be kept in contact with the area of treatment. The irradiation wavelength is 635 nm or 652 nm, with a fluence rate of up 200 $mWcm^{-2}$ [30].

1.4.4 Lasers

A laser (from the acronym Light Amplification by Stimulated Emission of Radiation) is an optical source that emits photons in a coherent beam [30]. Lasers have certain characteristics that make them especially suitable for use in PDT. Lasers are able to deliver intense light with a high degree of monochromaticity, which makes the focusing of the light beam into an optical fiber possible without a great loss of energy.

The employment of optical fibers in PDT enables treatment of internal tumors endoscopically and placement of the light source interstitially into the tumor tissue. The high power of laser light is of minor importance in PDT, because the light is used for photosensitizer activation and not for tissue incision by strong heating. The use of lasers as light sources has drawbacks, because they are expensive, complicated devices, which are not readily transportable [6].

1.5 Heavy atom effect in PDT

As singlet oxygen is the key cytotoxic agent in the PDT therapeutic process. The quantity of singlet oxygen generated by a photosensitizer is regulated by the efficiency of a spin-forbidden electronic transition from a singlet to a triplet state (ISC). The introduction of a heavy atom into a molecule is known to have an influence over the rates of the ISC and is termed the heavy-atom effect [33].

Introduction of a heavy metal ion strongly affects intersystem crossing in the complex via enhancement of spin-orbit coupling, which influences the formation and decay of triplet states. As a result, the rate of intersystem crossing is enhanced [7]. An electronic transition from a singlet to a triplet excited state within a molecule is a spin-forbidden process and as such occurs inefficiently for many compounds. In order for a transition between states of different spin multiplicities to occur effectively, a spin-orbit perturbation is generally required [34]. Enhanced spin-orbit perturbations can be achieved by the attachment of a heavy atom directly onto the molecule [35] (internal heavy-atom effect) or placing the molecule in a surrounding environment containing heavy atoms [36] (external heavy-atom effect).

O'Shea et al. have studied heavy atom effect on their work for singlet oxygen generation. They described a totally new class of PDT agent, the BF_2-chelated 3,5-diaryl-1H-pyrrol-2-yl-3,5diarylpyrrol-2-ylideneamines (tetraarylazadipyrromethenes). Photosensitizer singlet-oxygen generation level was modulated by the exploitation of the heavy atom effect. An array of photosensitizers with and without bromine atom substituents gave rise to a series of compounds with varying singlet-oxygen generation profiles (Figure 13).

In an attempt to effect varying degrees of spin-orbit coupling, they placed the heavy atoms at two different positions in the molecule. This allowed them to modulate the degree of spin-orbit coupling and hence the efficiency of singlet oxygen production by three modes: (i) no heavy atom within the sensitizer, thereby relying on the inherent spin-orbit coupling of the molecule; (ii) positioning of bromines on the aryl rings (not directly on the sensitizer), which could give rise to an intermediate singlet-oxygen generation level (termed an intramolecular external heavy-atom effect); and (iii) positioning of the bromine directly onto the sensitizer, thereby fully exploiting the internal heavy-atom effect and providing the most efficient singlet-oxygen producers (Figure 13).

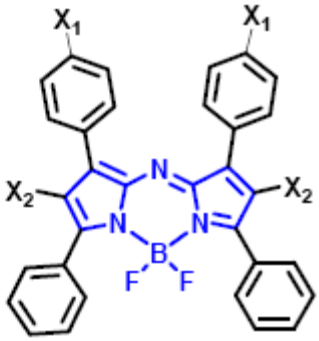

15

(i) X^1,X^2= H:inherent spin-orbit coupling
(ii) X^1= Br, X^2=H: itramolecular external heavy atom effect
(iii) X^1=H, X^2=Br: internal heavy atom effect

Figure 13. Positioning of the bromine heavy atom around the core sensitizer

The final step of the singlet-oxygen generation process is an energy transfer from photosensitizer triplet state to ground-state oxygen. An additional consequence of introducing heavy-atom substituents can be to give rise to nonradiative internal back conversion to the ground state or inhibiting the photosensitizer triplet to ground-state oxygen energy transfer. These competing pathways would give rise to loss of the excited-state energy without the generation of singlet oxygen. This makes the position of the heavy-atom within the sensitizer critical, as the atom(s) must be positioned to have a substantial effect on the degree of spin-orbit coupling but not give rise to competing excited-state energy loss pathways. As such an heavy atom can promote an S_1 to T_1 transition , ISC, though it may not necessarily result in enhanced singlet-oxygen production. This is evidence that the heavy atom effect can be exploited to deliver controlled levels of the key cytotoxic agent for photosensitizer class. The dramatically enhanced singlet-oxygen production levels show that the inclusion of the heavy atom as a substituent directly onto the central core of the photosensitizer has achieved the desired aim and has not given rise to loss of excited-state energy by internal radiationless transitions [1].

1.6 Photophysical processes of a molecule

1.6.1 Excitation

Excitation involves promoting an electron residing in a low-energy molecular level to a higher level. The lifetime of excited species is low because several mechanisms exist whereby an excited molecule can give up its excess energy and relax to its ground state [37] (Figure 14).

1.6.2 Internal Conversion

Internal conversion is a non-radiative transition between two electronic states of the same spin multiplicity. Therefore, internal conversion from S_1 to S_0 compete with emission of photons (fluorescence) and intersystem crossing to the triplet state from which emission of photons (phosphorescence) can possibly be observed [38].

1.6.3 Fluorescence

Emission of photons accompanying the S_1 to S_0 relaxation is called fluorescence. The fluorescence spectrum is located at higher wavelengths (lower energy) than the absorption spectrum because of the energy loss in the excited state due to the vibrational relaxation [38].

1.6.4 Intersystem crossing

Intersystem crossing is a non-radiative transition between two isoenergetic vibrational levels belonging to electronic states of different multiplicities. Crossing between states of different multiplicity is in principle forbidden, but spin-orbit coupling (i.e. coupling between the orbital magnetic moment and the spin magnetic moment) can be large enough to make it possible. The probability of intersystem crossing depends on the singlet and triplet states involved. It should also be noted that the presence of heavy atoms (i.e. whose atomic number is large, for example Br, Pb) increases spin-orbit coupling and thus favors intersystem crossing [38].

1.6.5 Phosphorescence

In solution at room temperature, non-radiative de-activation from the triplet state T_1, is predominant over radiative de-activation called phosphorescence. In fact, the transition T_1 to S_0 is forbidden (but it can be observed because of spin-orbit coupling), and the radiative rate constant is thus very low. The life time of the triplet state, may under these conditions, is long enough to observe phosphorescence on a time-scale up to seconds, even minutes or more [38].

1.6.6 Quantum yield

The tendency of a photosensitizer to reach the triplet state is measured by the triplet state quantum yield, which measures the probability of formation of the triplet state

per photon absorbed. The triplet state lifetime influences the amount of cytotoxic species which can be produced by collision-induced energy transfer to molecular oxygen and other cellular components [3].

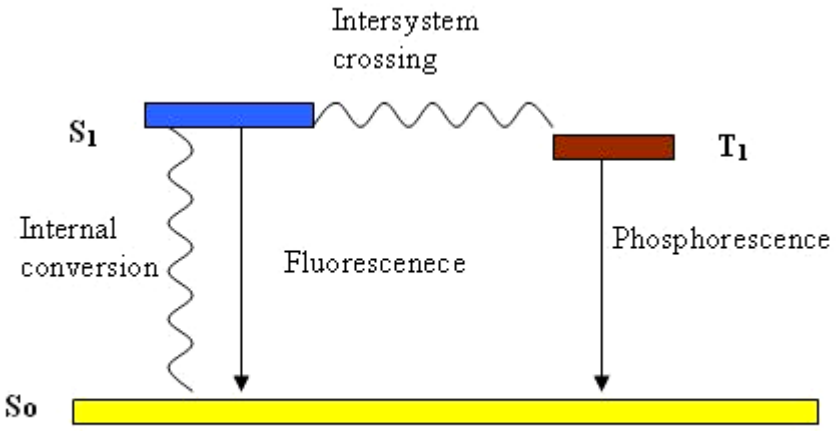

Figure 14. Simplified Jablonski diagram

1.7 PET (Photoinduced Electron Transfer)

PET dyes consist of a guest binding site (receptor) and a photon-interaction site (fluorophore). These two moieties are spatially separated from each other by an inert, -bounded spacer, therefore long range interactions between receptor and fluorophore are the reason for their communication. An electron transfer can be observed from the ion-free receptor to the fluorophore by strong long range interactions in the photoexcited state.

The PET (photoinduced electron transfer) effect observed in certain dyes has gained substantial interest for sensor development. PET-dyes show a substantial variation of the fluorescence intensity with pH, depending on whether the amino group is protonated or not, whereas absorption and shape of the spectra remain pH-invariant. Whether a PET occurs or not depends on several factors, such as redox potential of ground and excited states of the fluorophore and the receptor. Besides, the rate of PET is known to be strongly influenced not only by the electronic structure but also by solvent polarity.

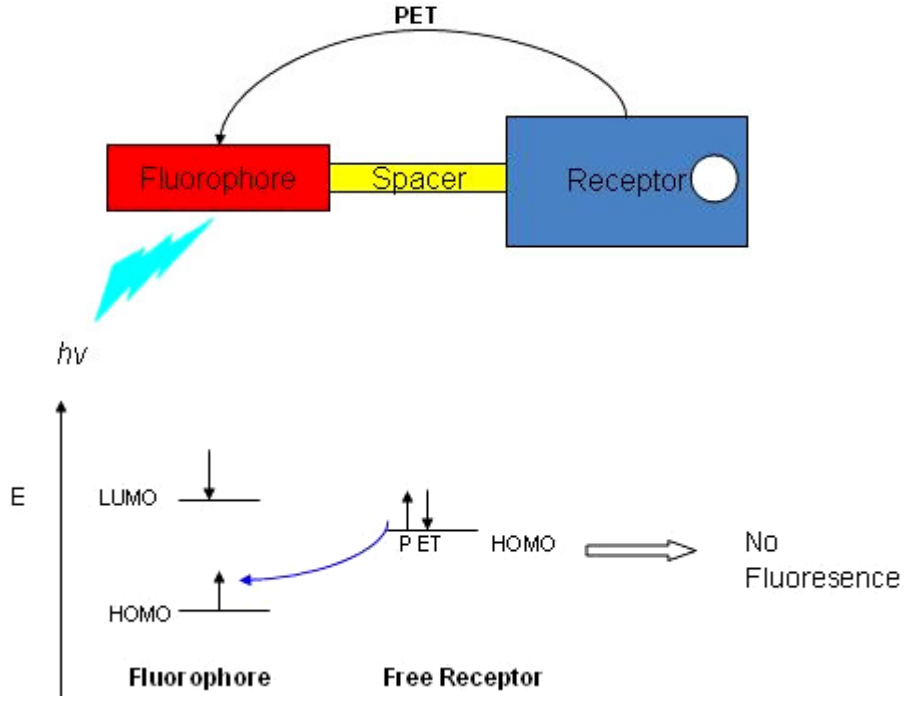

Figure 15. Spaced fluorophore-receptor system and representive frontier orbital energy diagram in the " off '' state.

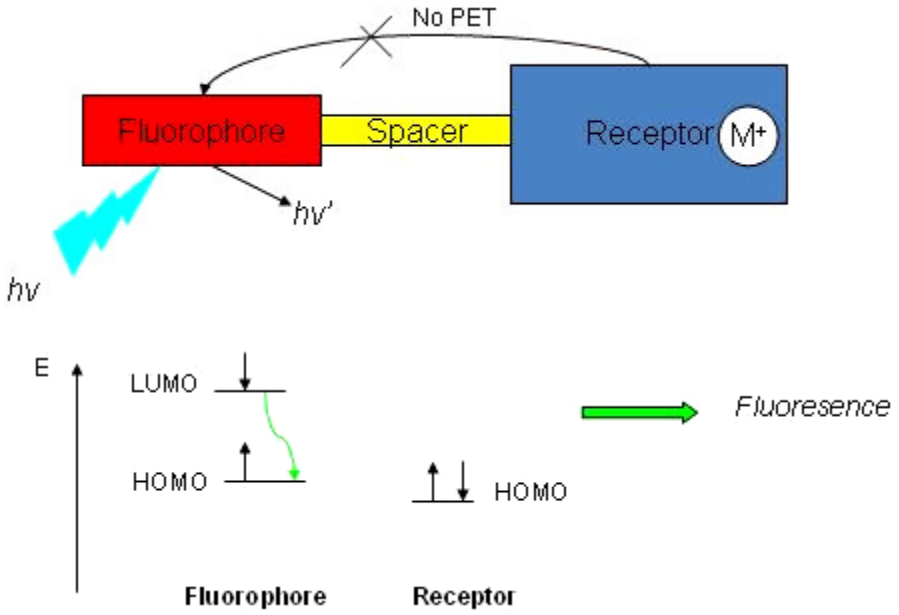

Figure 16. Spaced fluorophore-receptor system and representive frontier orbital energy diagram in the " on '' state.

Fluorescent signaling via the PET strategy is distinguished by its intrinsically supramolecular nature since distinct components perform each one (or more) of the necessary functions. A fluorophore module is the site of both photonic transactions of excitation and emission. A receptor module is responsible for guest complexation and decomplexation. A spacer module holds the fluorophore and receptor close to, but separate from each other. This also means that true molecular engineering applies, i.e., the optical, guest-binding, and redox properties of the components allow the quantitative prediction of the signaling parameters of the supramolecular system. Further, PET signaling systems have guest-induced "off-on" and "on-off" fluorescence. The pionering work of Weller over a quarter of a century is the starting point, since this provides the thermodynamic basis of PET. Figures **15** and **16** provide a summary in terms of frontier orbital energies. It also shows how PET systems employ thermal back-electron transfer as a self-repair mechanism following the potentially damaging PET process [39].

Several of the laboratories active in this field have summarized their own contributions along with related material. These include the groups of Czarnik, Fabbrizzi, Tsien, Kuhn, Rettig, Valeur and Shinkai [39]. Compound **16** is the simplest and first PET sensor which has been synthesized by de Silva et al., its fluorescence quantum yield increases from 0.003 to0.140 upon binding of K^+ in methanol solution [40] .

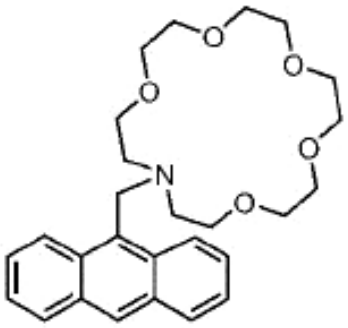

16

Figure 17. Crown containing fluorescent PET sensor **16**.

1.8 Advantages and limitations of photodynamic therapy

The most important application of PDT is in treatment of cancer. PDT has many advantages as compared with the traditional cancer treatments. It is a selective treatment that does not destroy healthy tissues. It is an effective, non-invasive treatment, which is at its best easy, fast, and painless to the patient. There are no serious side effects and no resistance normally develops, so that the treatment can be repeated if necessary. There is also no cross-resistance with other cancer treatments. It can be used to treat many different kinds of cancers, including cancers resistant to other treatments, and its efficacy is not dependent on the cell cycle phase.

Tissues treated by PDT also heal well, probably because the collagen they contain is not sensitive to photodynamic damage. The mechanical strength of tissues is mostly maintained and their perforation is therefore unlikely. Further, because most photosensitizers do not accumulate in the nuclei of normal cells, photodynamic damage is unlikely. The risk of carcinogenesis or mutations is therefore small. Light of wavelengths absorbed by the photosensitizer is needed for photodynamic action. Light that is normally used in PDT does not penetrate deep into tissue, as it is scattered and absorbed by endogenous chromophores. Therefore, PDT can be applied to treat tumors that are at the most 2 cm thick, the precise thickness depending on the photosensitizer used. Such tumors include cutaneous tumors and early stages of various other tumors.

PDT cannot be used when the destruction of the tumor would lead to a serious medical crisis, as when the tumor forms a part of the chest wall. PDT can, however, be combined with surgery; the tumor can be resected to a PDT treatable size, or PDT can be applied to remove possible microscopic remains of the tumor after surgery. It may also be combined with chemotherapy, radiation or hyperthermia. It can be used for palliation, where the goal is to reduce the size of the tumor and thereby alleviate the symptoms and increase the life expectancy of a terminal patient [6].

1.9 Logic gates

Logic gates are the workhorses of modern information technology, because computation relies on arithmetic and logic units. Arithmetic units can be dissected into simpler logic gate arrays. So, the challange is to pass on these properties and capabilities to molecules. This challenge has been accepted with increasing frequency since 1993, when it was demonstrated that molecular fluorescence signals can be switched under the influence of simple chemical species. The forces that drive research in molecular logic gates are identified as neutral science and computer technology. The longest established design relies on chemical inputs (usually ionic) and fluorescence outputs.

Despite a lot of efforts and expectations, molecular-scale electronics/photonics is undergoing a gradual evolution via wires, switches, and diodes with logic gates being beyond the current horizon. On the other hand, it has been possible to shift directly to molecular logic gates by combining chemical and photonic signals according to principles of supramolecular chemistry. Both our brains and modern silicon-based electronics technology rely heavily on integration [41].

1.9.1 Single-Input Molecular Logic

There are four possible output patterns arising from a single input. If the input is 0, the output can be 0 or 1 (two choices). If the input is 1, the output can again be 0 or 1 (two choices). Each one of these four output bit patterns corresponds to a logic type: PASS 0, YES, NOT and PASS 1. PASS 0 always outputs 0, whatever the input. PASS 1 always outputs 1. YES obediently follows the input (e.g., output 1 if input is 1). NOT always opposes the input (e.g., output 0 if input is 1). For instance, a NOT gate with a chemical input, fluorescence light output and excitation light for the power supply is 1 [43] (Figure 18). Any case of chemical-induced fluorescence quenching (of which there are hundreds) would have served in its place, testifying to the generality of this approach.

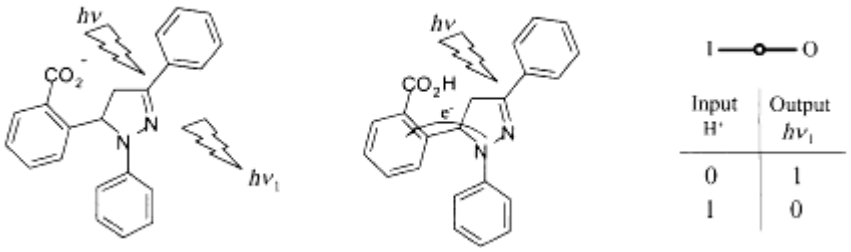

17

Figure 18. The molecular NOT logic gate **17**; principles of operation and truth table.

The H^+-induced fluorescence quenching arises as follows. When the H^+ level is low (input 0), excitation of the fluorophore results in bright fluorescence (output 1) with no substantial photochemistry intervening. However when the H^+ level is high (input 1), excitation of the fluorophore leads to photochemical intervention and, hence, the fluorescence is quenched (output 0). This intervention is photoinduced electron transfer (PET)]from the fluorophore to the protonated benzoate receptor (a rather electron-deficient unit).

1.9.2 Multiple-Input Molecular Logic

In Multiple-Input Molecular Logic, when the number of inputs is increased from 1 to 2, the possible number of logic types will rise to 16 [43].

Table 1. Truth table for some 2-input systems.

INPUTS		**OUTPUTS**			
A	**B**	**AND**	**NAND**	**OR**	**INHIBIT**
0	0	0	1	0	0
0	1	0	1	1	0
1	0	0	1	1	1
1	1	1	0	1	0

1.9.2.1 AND gate

AND logic, gives an output of 1 only if both inputs are 1. Since the first report of molecular AND logic gate by de Silva et al., many individual logic gates have been described on the basis of the spectral variations of molecular systems in response to external stimulations [44]. A molecular-scale example of this is from de Silva's group again, **18** (Figure 19). This AND gate is made possible by utilising two discrete, selective binding sites that are weakly coupled to a fluorophore. In this scheme, thermodynamically controlled and guest-modulated PET processes from oxidizable moieties located at each receptor serve to quench the fluorescence from the excited fluorophore, across inert methylene spacers. Only if chemical species (Na^+ and H^+) are present at both receptor1 and receptor2 are both oxidation potentials raised, such that the electron transfer is diminished. Then the fluorescence output is restored (output 1), and the truth table is satisfied. In this implementation, the power supply was provided by excitation light, while inputs are chemical (Na^+ and H^+) and the output is fluorescence light [45].

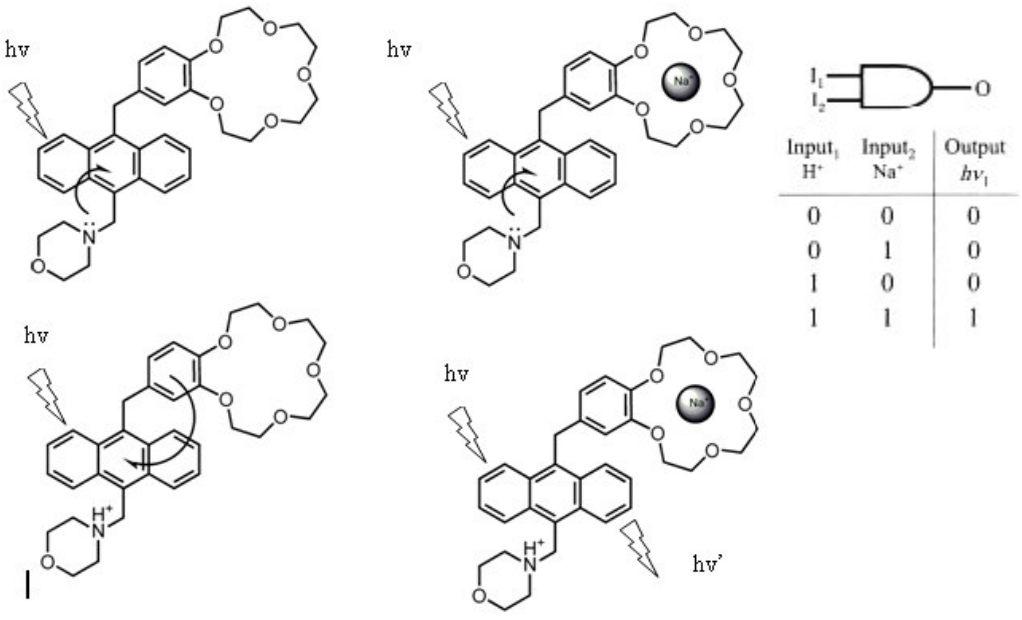

18

Figure 19. The molecular AND logic gate **18**: principles of operation and truth table.

1.9.2.2 OR gate

Another common 2-input logic type, OR, has been provided by Desvergne and Tucker (Figure 20), whereby the quantum yield of intramolecular photodimerization of two anthracene moieties is considered as the output. Quantum yield enhancement originates from the guest-enforced steric changes upon binding ions (Na^+ and Hg^{2+}) at either or both available sites (the 2,2'-bipyridine site or the flexible oligooxyethylene chains), giving an orientation conducive to photodimerization [46].

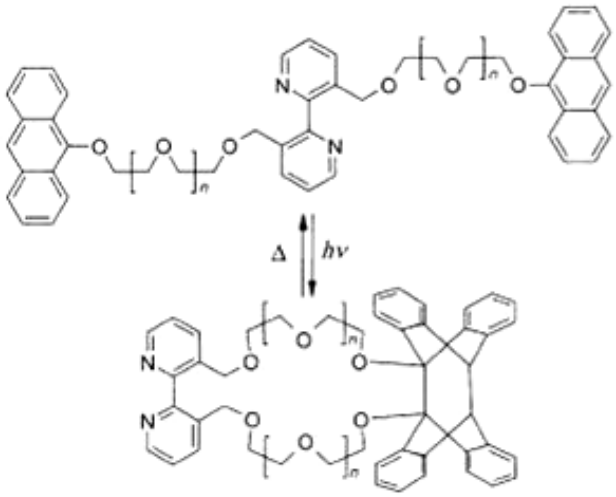

19

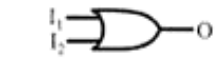

$Input_1$ Hg^{2+}	$Input_2$ Na^+	Output ϕ
0	0	0
0	1	1
1	0	1
1	1	1

Figure 20. Photoactive molecular system corresponding to an OR gate **19**.

1.9.2.3 INHIBIT gate

INHIBIT logic is another type that deserves some attention because it demonstrates noncommutative behaviour. This means that one input has the power to disable the whole system. Molecule **20** represents a different approache using a phosphorescence output. In a 2-input example, Gunnlaugsson et al. use a luminescent Tb^{3+} complex (Figure 21). Molecular oxygen is one input that quenches the delayed line-like emission, giving an output 0 regardless of the other inputs. The role of the second

input (H+) is to shift the absorption band of **20** into the range of the excitation light that provides the power for this device. Luminescence (output 1) is only observed if O_2 is absent (input 0), in the presence of acid (input 1) [47].

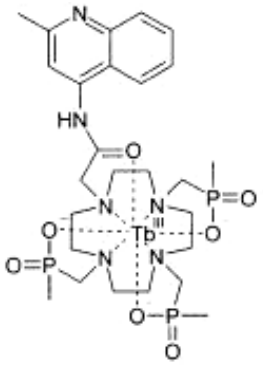

20

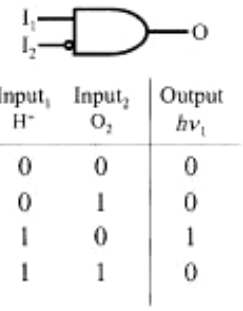

$Input_1$ H^+	$Input_2$ O_2	Output $h\nu_1$
0	0	0
0	1	0
1	0	1
1	1	0

Figure 21. Photoactive molecular system corresponding to an INHIBIT gate **20**.

1.9.2.4 NAND gate

NAND gates have high value in electronics, since multiple copies of these can be wired up to emulate all the other logic types. Akkaya and Baytekin use of a well-known compound **21** is of particular interest (Figure 22). They use hydrogen-bonding interactions for the first time alongside luminescence ideas for logic design with small molecules. Molecule **21** is known to intercalate into adenine (A)-thymine (T) base-pair regions of DNA. In aqueous/organic solvent mixtures they observe binding between the A-T mononucleotide pair and **21**, with the binding being signalled by luminescence spectral changes. Careful choice of emission wavelength (455 nm) shows significant reduction of luminescence intensity only when both A and T are present, that is, NAND logic [48].

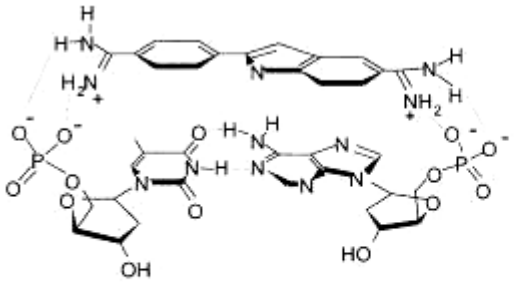

21

Input$_1$ A	Input$_2$ T	Output $h\nu_1$
0	0	1
0	1	1
1	0	1
1	1	0

Figure 22. Photoactive molecular system corresponding to an NAND gate **21**.

2. EXPERIMENTAL PROCEDURES

2.1 General

All chemicals and solvents purchased from Aldrich were used without further purification. ^{1}H NMR and ^{13}C NMR spectra were recorded using a Bruker DPX-400 in $CDCl_3$ or DMSO-d_6 with TMS as internal reference. Absorption spectrometry was performed using a Varian spectrophotometer. Column chromatography of all products was performed using Merck Silica Gel 60 (particle size: 0.040–0.063 mm, 230–400 mesh ASTM). Reactions were monitored by thin layer chromatography using fluorescent coated aluminum sheets. Solvents used for spectroscopy experiments were spectrophotometric grade. HRMS (FAB) measurements were done at the Kent Mass Spectrometry Laboratory, Kent, U.K.

2.2 Singlet Oxygen Measurements

Singlet Oxygen generation capacity of compound **26** was mesured in a dark room without any exposure to sunlight. Before each measurements the stock solution was aerated for 15 minute. During each measurement (0, 5, 10, 15, 20, 25, 30 min exposure to light) a 660 nm lead suorce, 3000 mCd, with a 7 cm cell distane to exposed light is used.

2.3 Synthesis of benzo-15-crown[5]

Pyrocatechol (35 mmol, 3.81 g), di-p-toluenesulfonate (35 mmol, 17.39 g), Na_2CO_3 (70 mmol, 7.34 g) were dissolved in 200 ml CH_3CN and refluxed for 48 h, then acetonitrile is evaporated in *vacuo*. The crude product was dissolved in chloroform and washed three times with water (in which KOH is dissolved). The chloroform layer is taken, dried over Na_2SO_3 and concentrated in *vacuo*. The crude prodact was purified by

silica gel column chromatography (eluent 93 $CHCl_3$: 7 MeOH). First fraction was collected (1.1 g, 11.7 %)

^{1}H NMR (400 MHz, $CDCl_3$) δ; 6.83-6.78 (m, 4H), 4.05 (t, J= 4.43 Hz, 4H), 3.82 (t, J= 4.35 Hz, 4H), 3.68 (s, 8H).

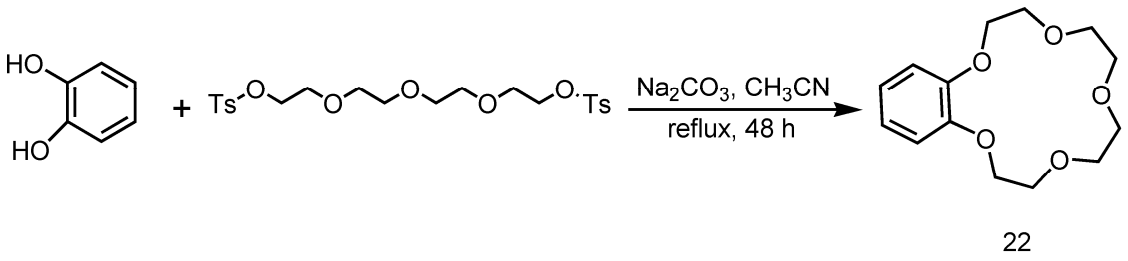

Figure 23. Tosylation reaction of catechol.

2.4 Synthesis of 4-formyl benzo-15-crown[5]

Compound **22** (4.10 mmol, 1.1 g) and hexamethylenetetramine (4.41 mmol, 0.618 g) were mixed with trifluoroaceticacid (6 ml). The reaction mixture was heated to 100 ^oC and kept at this temperature for 24 h. The dark red mixture was cooled to 5 ^oC, mixed with ice and stirred for 1 h. The product was extracted with $CHCl_3$, and dried over Na_2SO_4. The concentrated residue was purified by silica gel column chromatography (eluent 95 $CHCl_3$: 5 MeOH). The target product was obtained in the first fraction (323 mg, 26.69%).

^{1}H NMR (400 MHz, $CDCl_3$) δ; 9.7 (s, 1H), 7.32-7.30 (m, 1H), 7.25-7.23 (m, 1H), 6.87-6.81 (m, 1H), 4.14-4.038 (m, 4H), 3.79-3.76 (m, 4H), 3.63 (s, 8H).

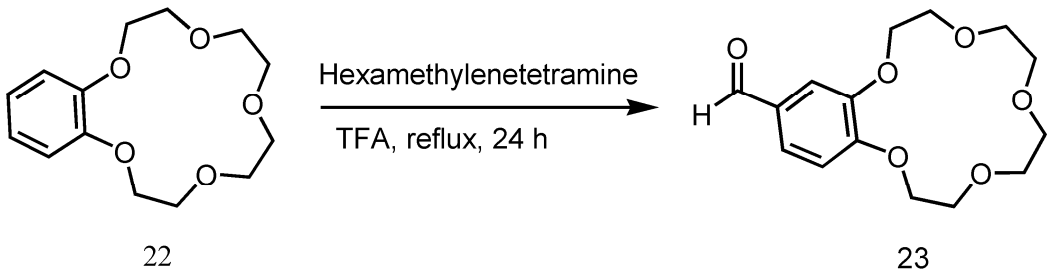

Figure 24. 4-formyl benzo-15-crown[5] production reaction from benzo-15-crown[5]

2.5 Synthesis of *meso*-Benzocrown appended BODIPY

Compound **23** (1.09 mmol, 323 mg) and 2, 4-dimethyl pyrole (2.20 mmol, 207 mg) were dissolved in 300 ml absolute CH_2Cl_2 (argon was bubled through CH_2Cl_2 for 30 min) under argon atmosphere. One drop of tfa was added and and the solution stirred at R. T until TLC control showed 50 % consumption (about 24 h) of aldehyde. At this point, a solution of tetrachlorobenzoquinone in 120 ml CH_2Cl_2 was added, stirring was continued for 30 min followed by the addition of 3 ml of Et_3N and 3 ml of BF_3OEt_2. After stirring for 30 min the reaction mixture was washed three times with water , dried over Na_2SO_4 and evaporated to dryness in *vacuo.* The residue was chromatographed on silica gel (95 $CHCl_3$: 5 MeOH) . The target product was obtained in the second fraction (277 mg, 49.4 %).

^{1}H NMR (400 MHz, $CDCl_3$) δ; 6.87 (d, J= 7.96 Hz, 1H), 6.71 (d, J= 11.55 Hz, 2H), 5.90 (s, 2H), 4.11 (t, J= 3.94 Hz, 2H), 4.01 (t, J= 4.02 Hz, 2H), 3.88 (t, J= 3.77 Hz, 2H), 3.83 (t, J= 4.11 Hz, 2H), 3.70 (d, J= 6.42 Hz, 8H), 2.47 (s, 6H), 1.40 (s, 6H) ;

^{13}C NMR (100 MHz, $CDCl_3$) δ; 155.3, 149.8, 143.2, 141.5, 131.7, 127.5, 121.1, 120.9, 113.9, 113.6, 71.0, 70.3, 69.4, 69.3, 69.0, 68.7, 61.0, 14.6, 14.5;

ESI-HRMS cald for [M+Na] 537.2354 found 537.2328 Δ=4.8 ppm.

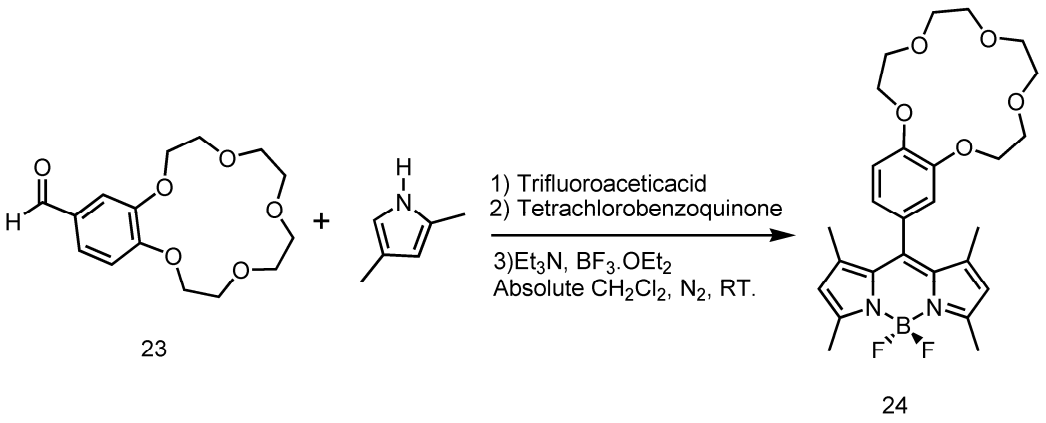

Figure 25. *Meso*-benzocrown appended BODIPY synthesis reaction.

2.6 Synthesis of 2,6-Diiodo-substituted BODIPY

HIO_3 (1.32 mmol, 232 mg) is dissolved in minimum amount of water and added dropwise to a solution of **24** (0.33 mmol, 170 mg) and I_2 (1.65 mmol, 419 mg) in 10 ml EtOH. The mixture was heated to 60 ^oC for 20 min. Then, cooled down to room temperature and extracted with sodium thiosulphate dissolved water and CH_2Cl_2. The organic phase was dried over Na_2SO_4 and concentrated in *vacuo*. Then crude product was purified by silica gel column chromatography (eluent 95 $CHCl_3$: 5 MeOH). The target product was obtained (95 mg, 37.5 %).

^1H NMR (400 MHz, $CDCl_3$) δ; 6.91 (d, J= 8.08 Hz, 1H), 6.71-6.66 (m, 2H), 4.11 (t, J= 4.07 Hz, 2H), 4.01 (t, J= 4.17 Hz, 2H), 3.88 (t, J= 4.05 Hz, 2H), 3.83 (t, J= 4.12 Hz, 2H), 3.72 (d, J= 7.35 Hz, 8H), 2.47 (s, 6H), 1.40 (s, 6H);

^{13}C NMR (100 MHz, $CDCl_3$) δ; 156.6, 150.1, 150.0, 145.4, 141.2, 131.6, 127.1, 120.8, 114.0, 113.3, 85.5, 71.0, 70.3, 70.2, 69.3, 69.2, 69.1, 68.7;

ESI-HRMS cald for [M+Na] 789.0286 found 789.0257 Δ=3.7 ppm.

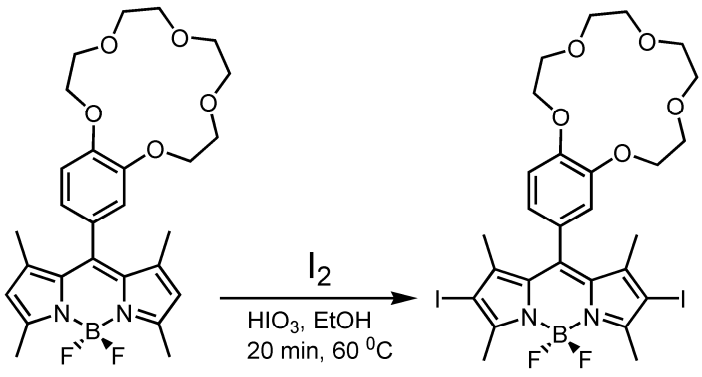

24 25

Figure 26. Iodination reaction of *meso*-benzocrown appended BODIPY.

2.7 Synthesis of target compound 26

Compound **25** (0.124 mmol, 95 mg) and 4-pyridinecarboxaldehyde (0.45 mmol, 53 mg) were refluxed for 20 min in a mixture of benzene (25 ml), piperidine (275 µl) and AcOH (230 µl). Any water formed during the reation, was removed azeotropically by heating the mixture in a Dean - Stark apparatus. The reaction was monitored by TLC (eluent 95 $CHCl_3$: 5 MeOH). Organic phase was washed three times with $NaHCO_3$ dissolved water, dried over Na_2SO_4 and concentrated in *vacuo*. The crude product was purified by silica gel column chromatography (eluted first with 95 $CHCl_3$: 5 MeOH then flash column chromatography of 1 EtOAc : 1 $CHCl_3$). The product was collected (15 mg, 12.8 %).

^{1}H NMR (400 MHz, $CDCl_3$) δ; 8.70-8.61 (m, 4H), 7.96 (d, J= 16.72 Hz, 2H), 7.73 (d, J= 16.73 Hz, 2H), 7.48-7.42 (m, 4H), 6.94 (d, J= 8.12 Hz, 1H), 6.78-6.72 (m, 2H), 4.25-4.11 (m, 2H), 4.06-4.03 (m, 2H), 4.06-4.03 (m, 2H), 3.94-3.88 (m, 2H), 3.75-3.68 (d, 8H), 1.51 (s, 6H) ;

ESI-HRMS cald for [M+Na] 967.0812 found 967.0776 Δ=3.7 ppm.

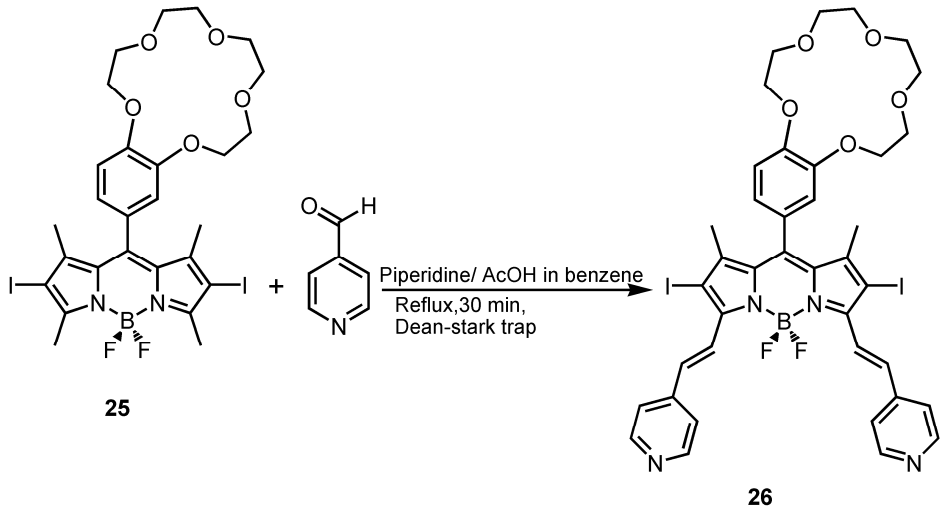

25 26

Figure 27. Formation of di-styrl pyridine unit on the bodipy framework.

3. RESULTS AND DISCUSSION

3.1 Generation of a novel photosensitizer: 3,5-di-styryl substituted boradiazaindacene dye

The design for the automaton includes the following elements; i) strong long wavelenght absorption preferably beyond 650 nm; 3,5-di-styryl substituted bodipy dyes are useful in this regard with typical absorption peaks ranging from 630-750 nm ii) an acid sensitive absorption peak; we reasoned this could be best achieved by incorporating di-methyl amino styryl or pyridyl ethenyl moities iii) in order to modulate PET efficiency and intersystem crossing efficiency which is directly related to the PET process, we utilized a crown ether based PET modulator which is only sensitive to sodium but not to hydrogen ions. With this design we set out for the synthesis of compound **26.**

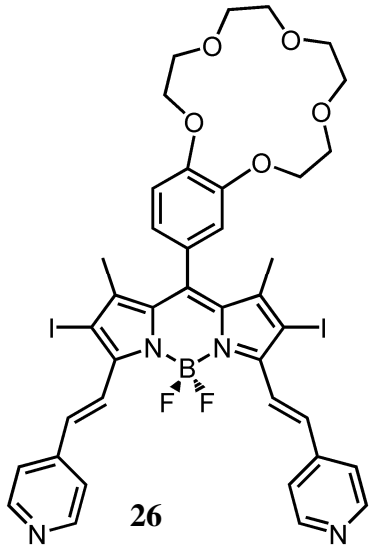

26

Figure 28. Chemical structure of the compound **26.**

Our synthesis starts with the formulation of benzo-15-crown[5]. Then, using standard procedures and the resulting aldehyde together with 2,4-dimethyl pyrole, a bodipy dye was obtained. To facilitate intersystem crossing 2 and 6 positions of the

boradiazaindacene ring system was iodinated with iodic acid-iodine mixture. Acid sensitivity conferring pyridyl groups were attached by a two-fold Knoevenagel reaction of three and five methyl groups and 4-pyridyl carboxy aldehyde. Spectral and singlet oxygen generation of compound **26** were studied in acetonitrile. When a small aliquote of TFA was added to acetonitrile solution of **26**, a red shift in the absorption spectra was observed moving the peak value from 630 to 660 nm. We have also demonstrated that this shift is produced only when acid was added, even large sodium concentrations did not cause any spectral shifts. The excitation source of our choice was a LED array with peak irradiation at 660 nm. This means that the dye **26** can only be excited under acidic conditions to generate singlet oxygen because only when pyridine groups are protonated, the compound becomes strongly absorbing at 660 nm.

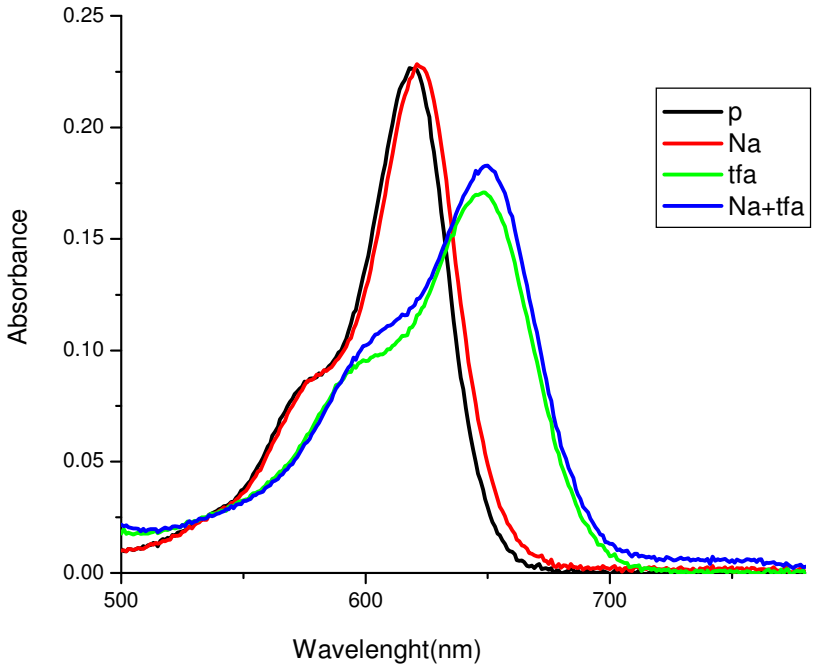

Figure 29. Absorbance spectra of target compound **26,** p (in the presence of just photosensitizer-target compound **26**), Na (in the presence of $NaClO_4$), TFA (in the presence of TFA), Na+TFA (in the presence of both $NaClO_4$ and TFA)

3.2 Singlet oxygen generation capacity of compound 26

Relative rates of singlet oxygen generation were determined using 1,3-diphenyl-iso-benzofuran as a trap molecule.

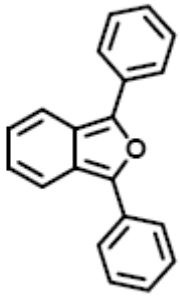

Figure 30 Structure of the singlet oxygen trap 1,3-diphenyl-isobenzofuran (DPBF).

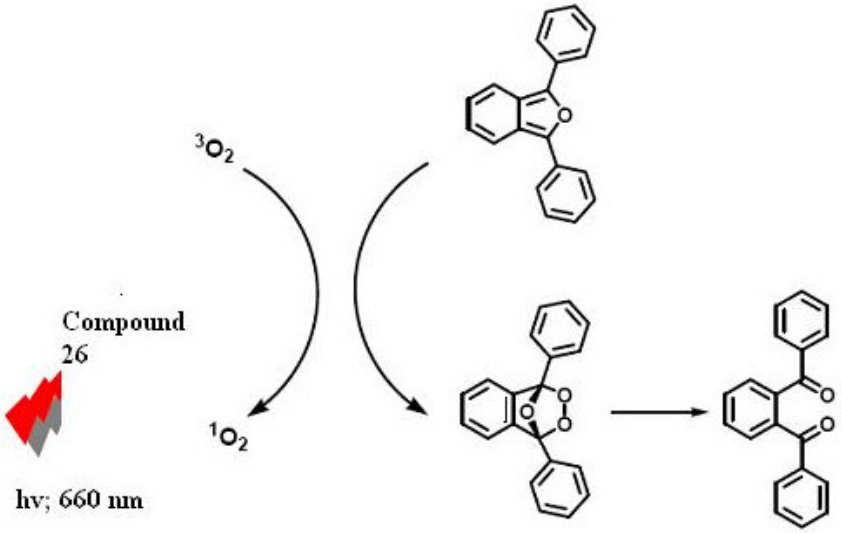

Figure 31. Excitation of compound **26** with LED light in air saturated solution causes a remarkable degradation of the selective singlet oxygen trap 1,3-diphenyl-iso-benzofuran.

A few years ago we have demonstrated that appropriately decorated bodipy dyes can be very efficient generators for singlet oxygen, thus act as a satisfactory photodynamic agents. As a bonus these dyes absorbed very strongly at 660 nm which is considered to be within the therapeutic window of mammalian tissue. So, combining our earlier experience in molecular logic gates and rational design of photodynamic agents, we proposed a photodynamic therapy agent that would release singlet oxygen at a much larger rate when the cancer related cellular parameters are above a threshold value at the same location. Thus, the proposed logic gate is an AND logic gate, the output of which is singlet oxygen. Following the survey of the relevant literature for cancer related parameters, we decided that sodium ion concentration and pH (H^+) concentration could be very promising targets. In the tumor regions the pH can drop below 6 and the Na^+ concentration is also significantly higher then normal tissues. As a result in the proposed logic system the chemical inputs could be Na^+ and H^+.

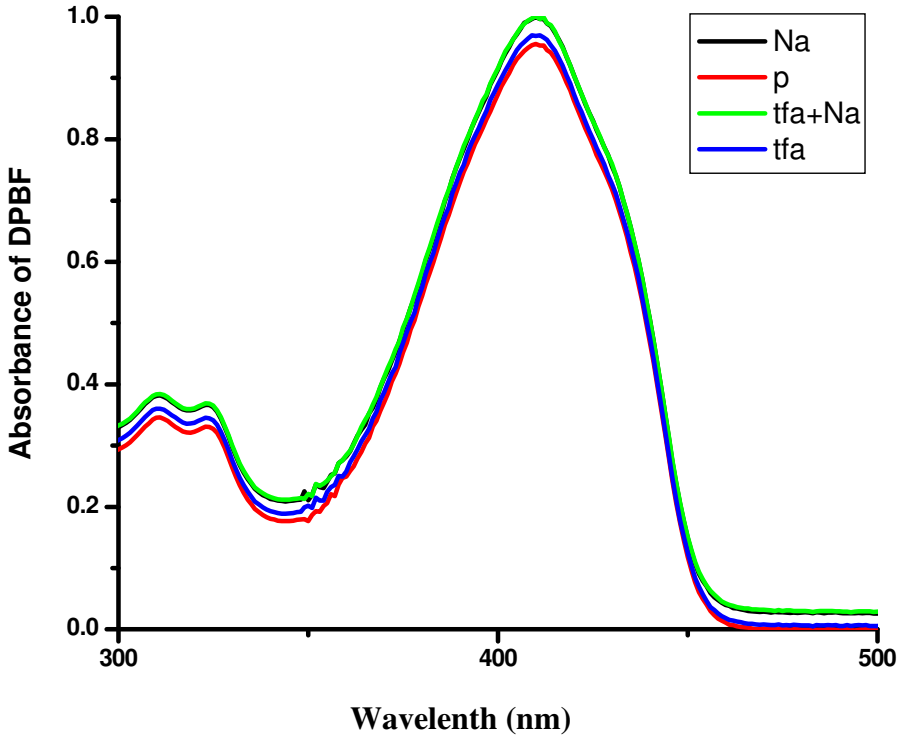

Figure 32. Absorbance spectra of 1,3-diphenyl-isobenzofuran (DPBF concentration 100 μM) in acetonitrile, without any exposure to 3000 mCd light in the presence of 10 nM photosensitizer (p) **26**, p (no Na^+ or TFA is added), Na (in the presence of 20 mM $NaClO_4$), TFA (in the presence of 1 μM TFA), Na^+ + TFA (in the presence of both 20 mM $NaClO_4$ and 1 μM TFA)

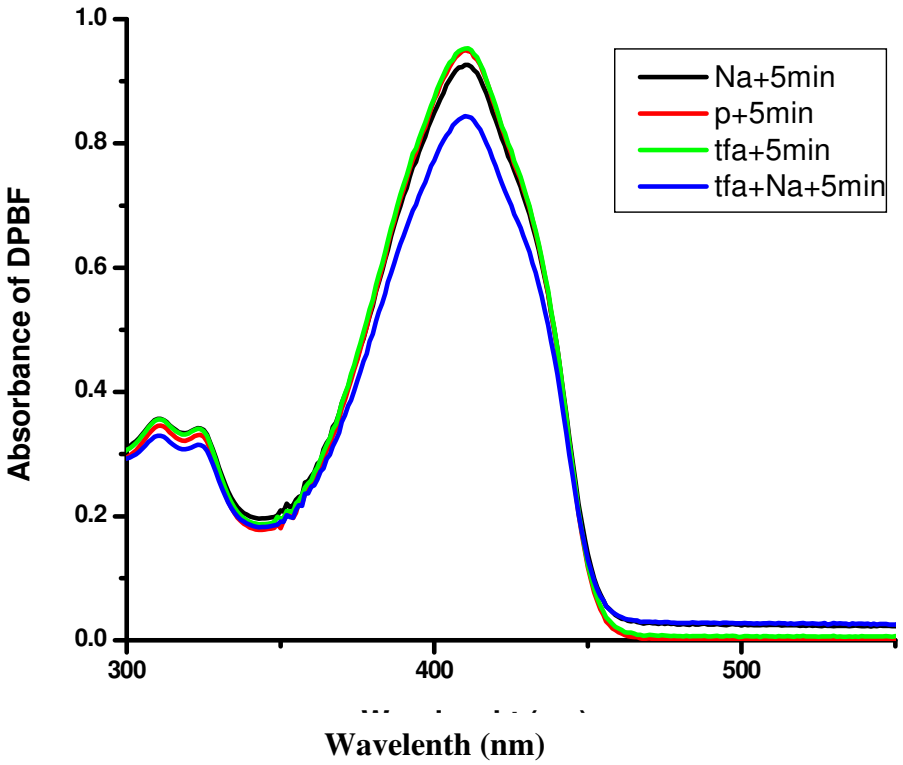

Figure 33. Absorbance spectra of 1,3-diphenyl-isobenzofuran (DPBF concentration 100 μM) in acetonitrile with 5 minute exposure to 3000 mCd light in the presence of 10 nM photosensitizer (p) **26**.

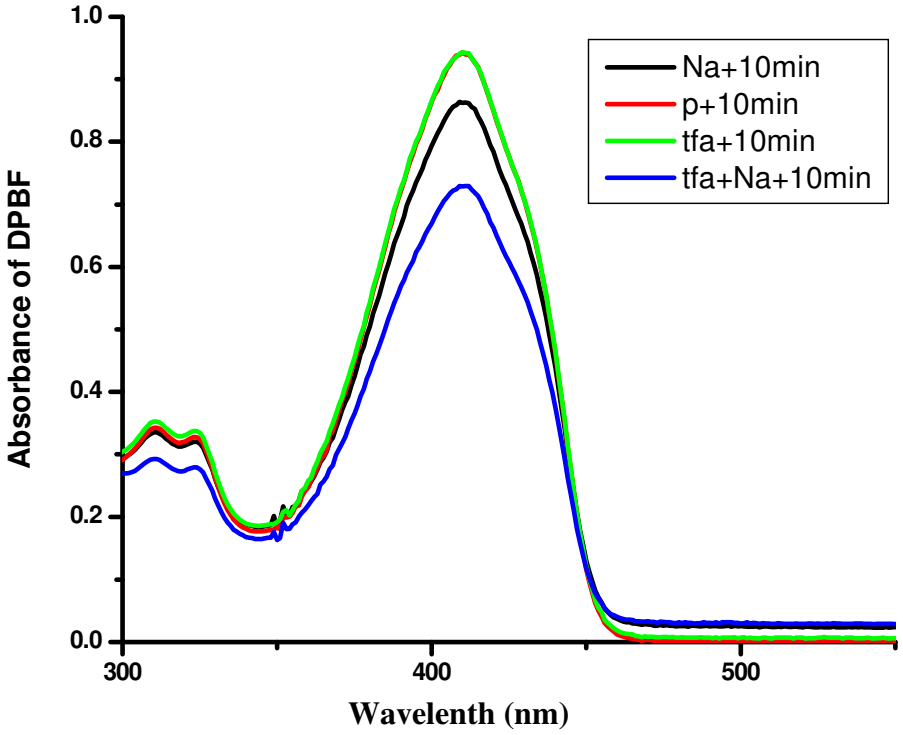

Figure 34. Absorbance spectra of 1,3-diphenyl-isobenzofuran (DPBF concentration 100 μM) in acetonitrile with 10 minute exposure to 3000 mCd light in the presence of 10 nM photosensitizer (p) **26**.

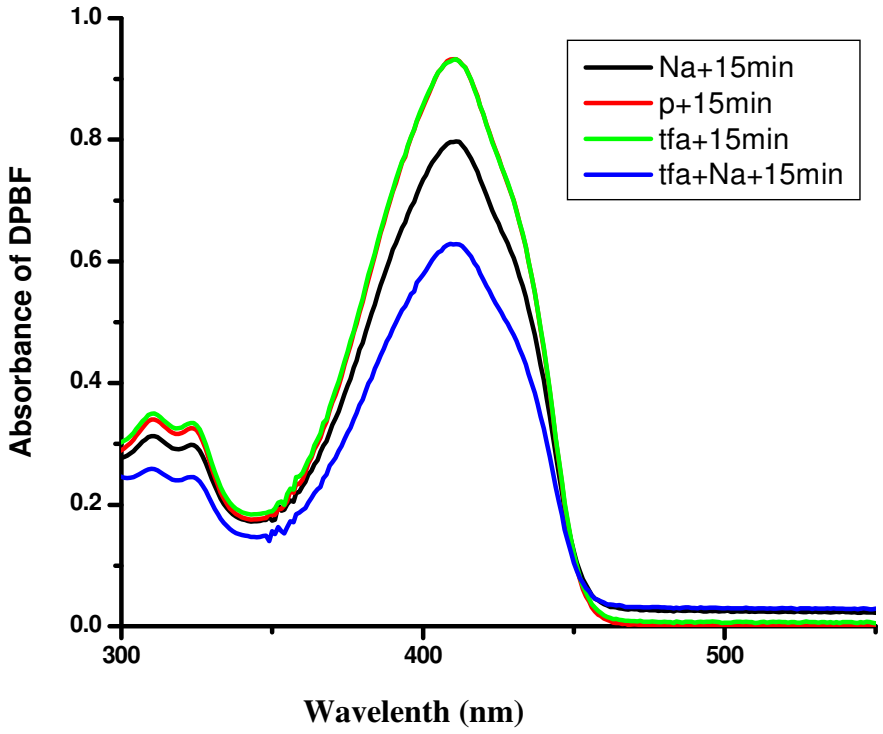

Figure 35. Absorbance spectra of 1,3-diphenyl-isobenzofuran (DPBF concentration 100 μM) in acetonitrile with 15 minute exposure to 3000 mCd light in the presence of 10 nM photosensitizer (p) **26**.

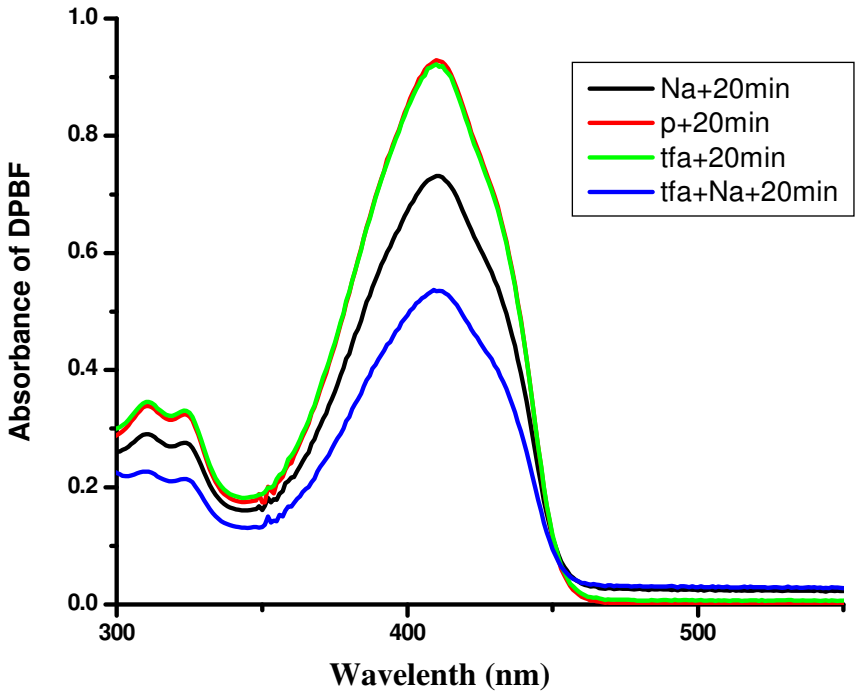

Figure 36. Absorbance spectra of 1,3-diphenyl-isobenzofuran (DPBF concentration 100 μM) in acetonitrile with 20 minute exposure to 3000 mCd light in the presence of 10 nM photosensitizer (p) **26**.

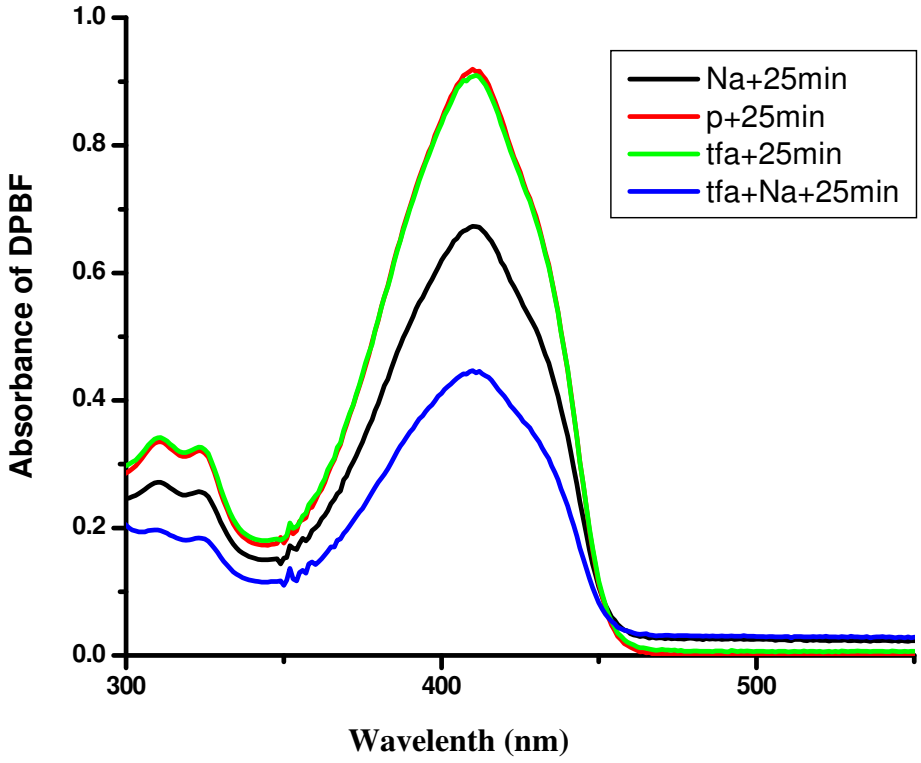

Figure 37. Absorbance spectra of 1,3-diphenyl-isobenzofuran (DPBF concentration 100 μM) in acetonitrile with 25 minute exposure to 3000 mCd light in the presence of 10 nM photosensitizer (p) **26**.

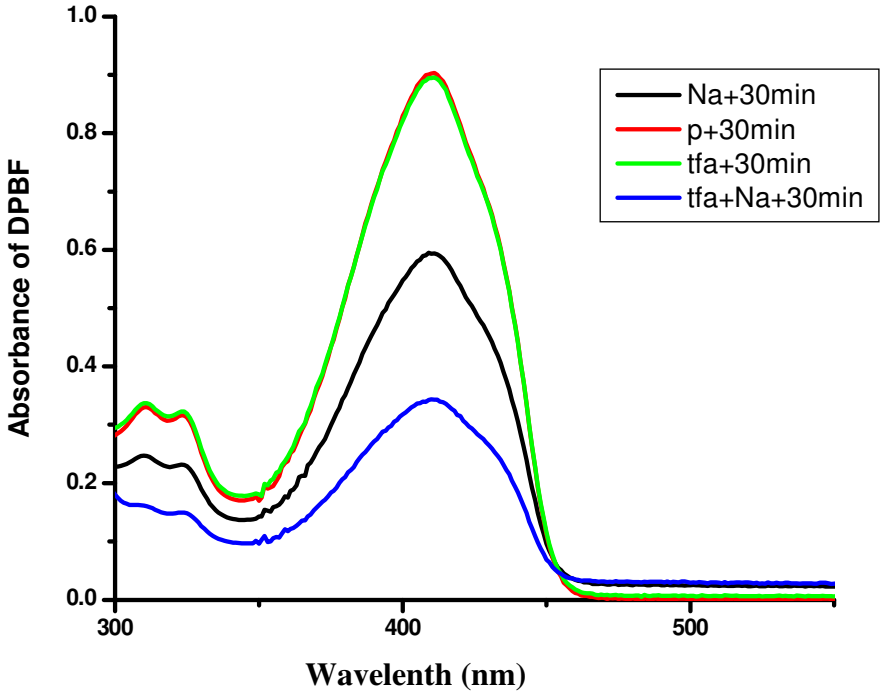

Figure 38. Absorbance spectra of 1,3-diphenyl-isobenzofuran (DPBF concentration 100 μM) in acetonitrile with 30 minute exposure to 3000 mCd light in the presence of 10 nM photosensitizer (p) **26**.

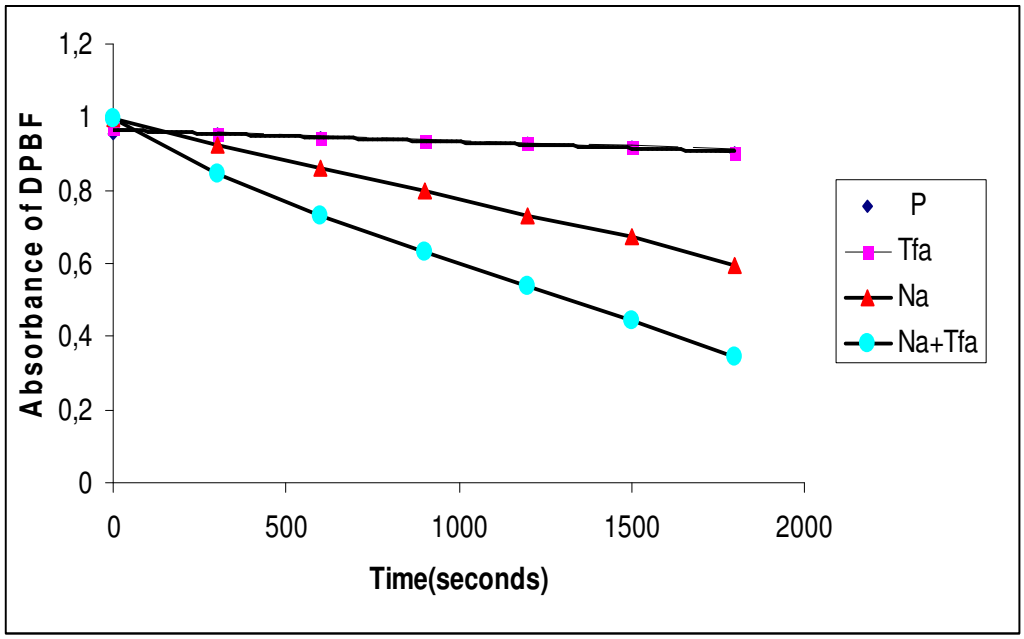

Figure 39. Absorbance of DPBF vs time graph with relative slopes.
Slopes; P = $3x10^{-5}$, tfa = $3x10^{-5}$, Na = $2x10^{-4}$, Na + tfa = $4x10^{-4}$.

During the 0, 5, 10, 15, 20, 25, 30 minute exposure of the sample to 660 nm LED source, the maximum decrease in 1,3 di-phenyl isobenzofuran absorption i.e.maximum rate of singlet oxygen generation were observed when both TFA and Na^+ ions were present . When neither TFA (H^+ ions) nor $NaClO_4$ (Na^+ ions) were present or when only TFA was present a very low rate of production is in effect. Na^+ alone results in a somewhat higher rate, demonstrating the reciprocal relationship between PET and intersystem crossing processes, at least for this molecule. This experimental results are in accordance with AND logic operation. The system in fact is an automaton which is to seek higher concentration of both hydrogen and sodium ions, and release the toxic agent (singlet oxygen) only when both concentrations are high.

Table 2. AND truth table and corresponding AND gate for compound **26**.

INPUT		OUTPUT
A	**B**	**A AND B**
0	0	0
1	0	0
0	1	0
1	1	1

INPUT		OUTPUT
Na^+	**H^+**	**$^1O_2$**
0	0	Low (1.0)
1	0	Low (6.6)
0	1	Low (1.0)
1	1	**High** (13. 3)

4. CONCLUSION

In this study a novel photosensitizer 3,5-di-styryl substituted boradiazaindacene dye was synthesized. This compound is a prototypic example of an automaton which releases its lethal weapon following an analysis of enviromental parameters for sign of disease and when necessary and sufficient conditions are met. This prototype also points to the direction of further development; incorporation of additional functional units which modulate singlet oxygen generation efficiency could result in therapeutic agents with very high level of selective delivery potential. The notion of molecular logic gates assisted us in the design of this particular PDT agent and it is very likely molecular medicine, could be the first niche application of molecule based logic gates.

REFERENCES

[1] Gorman A., Killoran J., O'Shea C., Kenna T., Gallagher W. M. and O'Shea D. F., J. Am. Chem. Soc., **2004**, 126, 10619–10631.

[2] Roy I., Ohulchanskyy T. Y., Pudavar H. E, Bergey E. J., Oseroff A. R., Morgan J., Dougherty T. J., Prasad P. N., J. Am. Chem. Soc**.** , **2003**, 125, 7860- 7865.

[3] Pushpan S. K., Venkatraman S., Anand V.G., Sankar J., Parmeswaran D., Ganesan S., Chandrashekar T.K., Curr. Med. Chem., **2002,** 2*,* 187-207.

[4] Epstein, J. M. N. Engl. J. Med., **1990**, 32, 1149-1151.

[5] Spikes J. D., Photochem. Photobiol., 65, **1997**, 142S-147S.

[6] Nyman E. S., Hynninen P. H., J. Photochem. Photobio. 73, **2004**, 1–28.

[7] Szacilowski, K., Macyk, M., Matuszek, A. D., Brindell, M., Stochel, G., Chm. Rev. 105, **2005**, 2647-2694.

[8] Morris R. L., Azizuddin K., Lam M., Berlin J., Nieminen A., Kenney M. E., Samia A. C. S., Burda C., Oleinick N. L., Cancer Res. **2003**, 63, 5194-5196.

[9] Allen C. M., Sharman W. M., Van Lier J. E., J. Porphyrins Pthalocyanines **2001**, 5, 161-163

[10] Ali H., van Lier, J. E. Chem. Rev. **1999**, 99, 2379-2381.

[11] Nyman E. S., Hynninen P. H., J. Photochem. Photobiol., B: Biol, **2004**, 73, 1-3.

[12] Capella M. A. M., Capella L. S., J. Biomed. Sci, **2003**, 10, 361-366

[13] Dougherty T. J., Crit. Rev. Oncol. Hematol., **1984**, 2, 83-85.

[14] Allison R. R., Downie G. H., Cuenca R., Hu X. H., Childs C. J. H., Sibata C. H., Photodiagn. Photodyn. Ther. **2004**, 1, 27-29.

[15] Sharman W. M., Allen C. M., van Lier J. E., Drug. Discuss. Today, **1999**, 4, 507-509.

[16] Brown S., Int. Photodyn., **1996**, 1, 1-3.

[17] Sobolev A. S., Stranadko E. F., Int. Photodyn., **1997**, 1, 2-4.

[18] Evenson J. F., Sommer S., Rimington C., Moan J. Br., J. Cancer, **1987**, 55, 483-485.

[19] Sternberg E. D., Dolphin D., Brückner C., Tet. Let., **1998,** 54**,** 4151-4202.

[20] Paquette B., Boyle R. W., Ali, H., MacLennan A. H., Truscott T. G., van Lier J. E. Sulfonated phthalimidomethyl aluminum phthalocyanine: The effect of hydrophobic substituents on the in vitro phototoxicity of phthalocyanines.

[21] Jori G., J. Photochem. Photobiol., **1992**, 62, 371-378.

[22] Wyss P., Schwarz V., Dobler-Girdziunaite D., Hornung R., Walt H., Degen A., Fehr M. K., Int. J. Cancer , **2001**, 93, 720- 724.

[23] Yukruk F., PhD thesis, METU, **2005.**

[24] Killoran J., Allen L., Gallapher J. F., Gallapher W. M., O'Shea D. F., Chem.Commun., **2002**, 1862-1863.

[25] Mc. Donell S. O., Hall M. J., Allen L. T., Byrne A., Gallagher W. M., O'Shea D. F., J. Am. Chem. Soc., **2005**, 127, 16360-16361.

[26] Karolin J., Johansson L. B. A., Strandberg L., Ny T., J. Am. Chem. Soc. **1994**, 116, 7801- 7806.

[27] Wittmershaus B. P., Skibicki J. J., McLafferty J. B., Zhang Y. Z., Swan S., J. Fluoresc., **2001**, 11, 119- 128.

[28] Yogo T., Urano Y., Ishitsuka Y., Maniwa F., Nagano T., J. Am. Chem. Soc. **2005**, 127, 12162- 12163.

[29] Atılgan S., Ekmekçi Z., Doğan A. L., Güç Dicle, Akkaya E. U., Chem. Commun.., **2006**, 4398-4400.

[30] Atılgan S., Ms Thesis, METU, **2006.**

[31] Baytekin H. T., Akkaya E. U., Org. Lett., **2000**, 2, 1725-1727.

[32] Dougherty T. J, Gomer C. J., Henderson B. W., Jori G., Kessel D., Korbelik M., Moan J., Peng Q., J. Natl. Cancer. Inst., **1998**, 90, 889-905.

[33] Turro N. J. In Modern Molecular Photochemistry; University Science Books: Sausalito, CA, **1991**, 191- 195.

[34] Lower S. K., El-Sayed M. A., Chem. Rev., **1966**, *66*, 199-201.

[35] Yuster P., Weissman S. I., J. Chem. Phys. **1949**, 17, 1182-1183.

[36] Koziar J. C., Cowan D. O., Acc. Chem. Res. **1978**, 334-336.

[37] Douglas A. Skoog, Donald M. West, F. James Holler, Fundamentals of Analytical Chemistry, **1996**, 506-508.

[38] Valeur B., Molecular fluorescence principles and applications, Wiley, **2001**, 34-47.

[39] De Silva A. P., Gunaratne H. Q. N., Gunnlaugsson T., Huxley A. J. M., McCoy C. P., Rademacher J. T., Rice T. E., Chem. Rev. **1997,** 97, 1515-1566.

[40] De Silva A. P., De Silva S.A., J. Chem. Soc. Chem. Commun., **1986**, 1709-1711.

[41] Atwood J. L., Steed J. W., Encyclopedia of Supramolecular Chemistry, **2000**, 893.

[42] De Silva A. P., De Silva S. A., Dissanayake A. S., Sandanayake K. R. A. S., J. Chem. Soc. Chem. Commun., **1989**, 1054 -1056.

[43] Ben-Ari M., Mathematical Logic for Computer Science, Prentice- Hall, Hemel Hempstead, **1993**.

[44] De Silva, A. P., Gunaratne H. Q. N., McCoy C. P., Nature (London), **1993**, *364*-366.

[45] De Silva A. P., Gunaratne H. Q. N., McCoy C. P., J. Am. Chem. Soc. **1997**, 119, 7891 -7892;

[46] McSkimming G., Tucker J. H. R., Bouas-Laurent H., Desvergne J. P., Angew. Chem., **2000**, 112, 2251-2253;

[47] Gunnlaugsson T., Mac Donail D. A., Perker D., Chem. Commun., **2000**, 93-94.

[48] Baytekin H. T., Akkaya E. U., Org. Lett. **2000**, 2, 1725 -1727.

APPENDIX

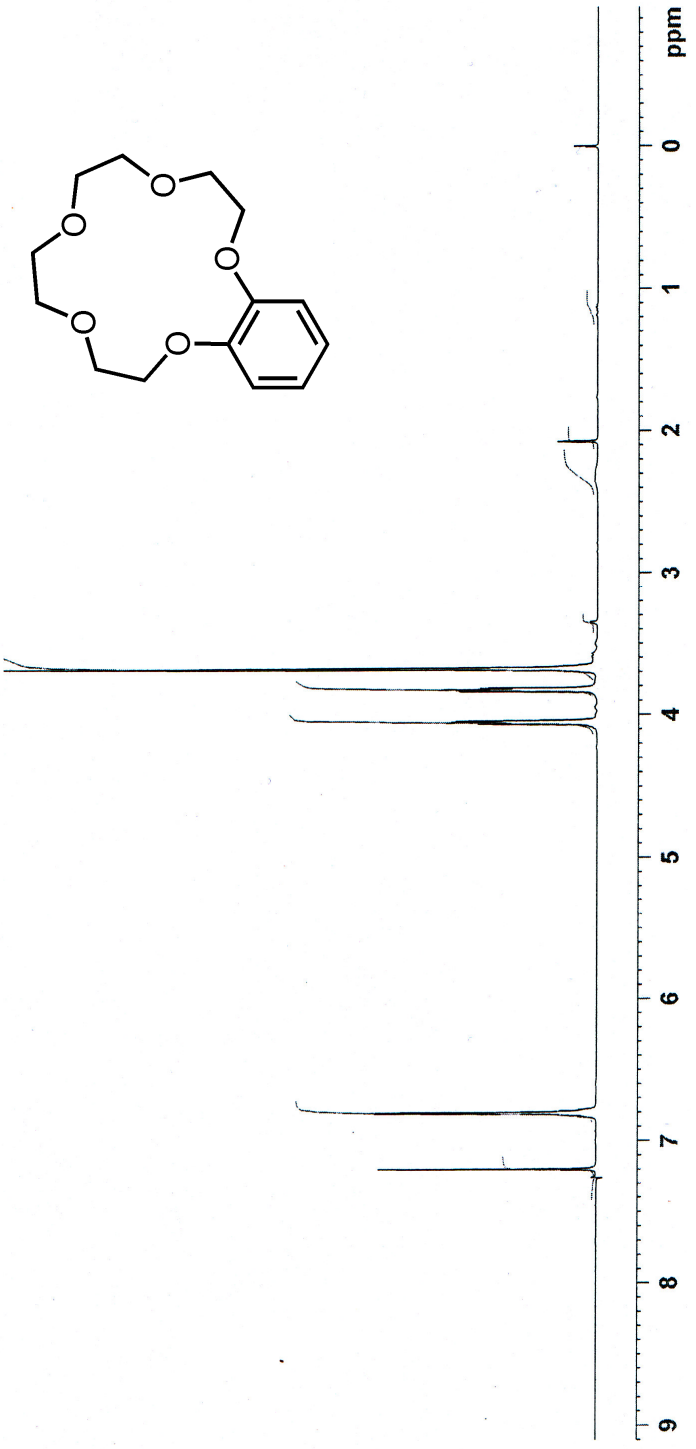

Figure 40 ^{1}H NMR spectra of compound **22**

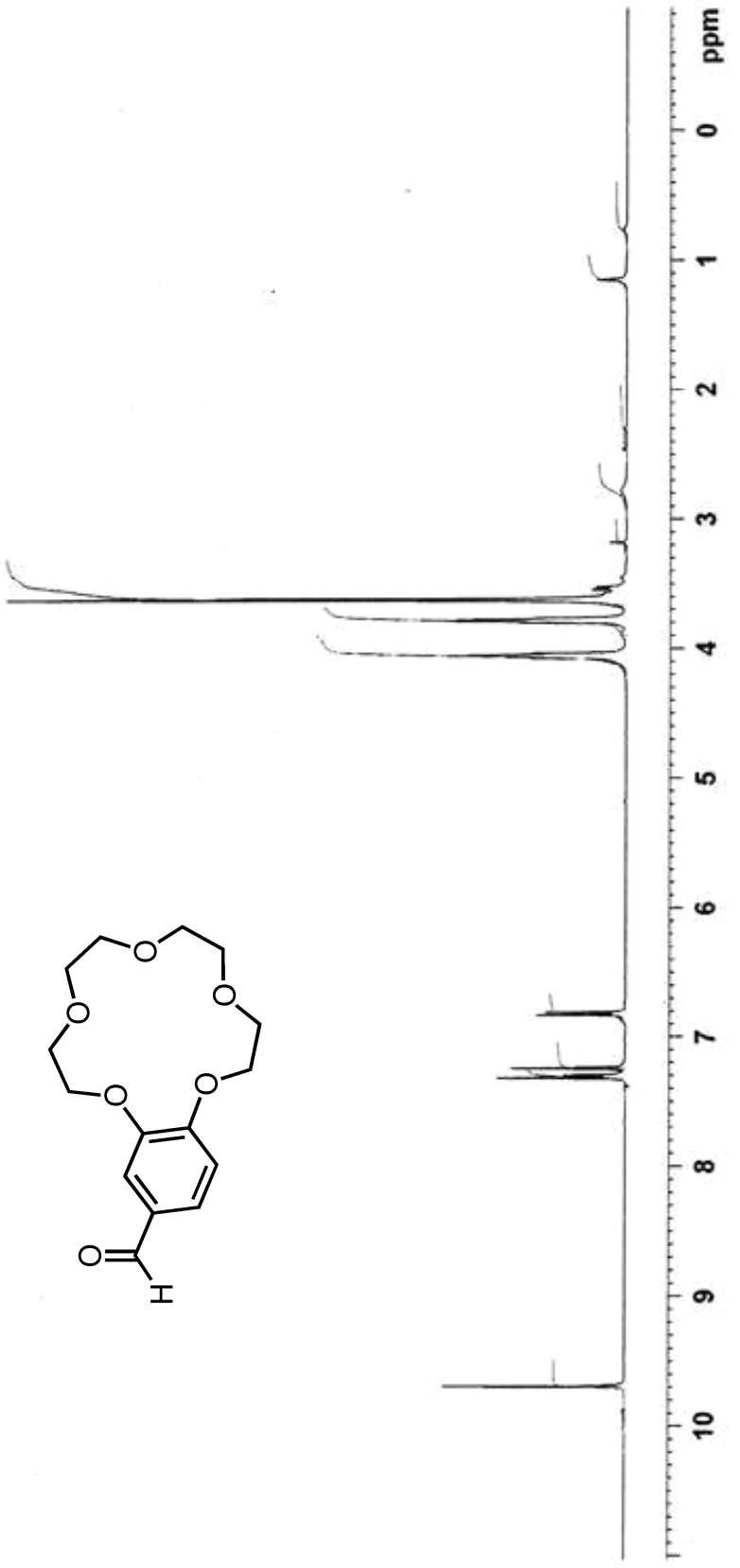

Figure 41 ^{1}H NMR Spectra of compound **23**

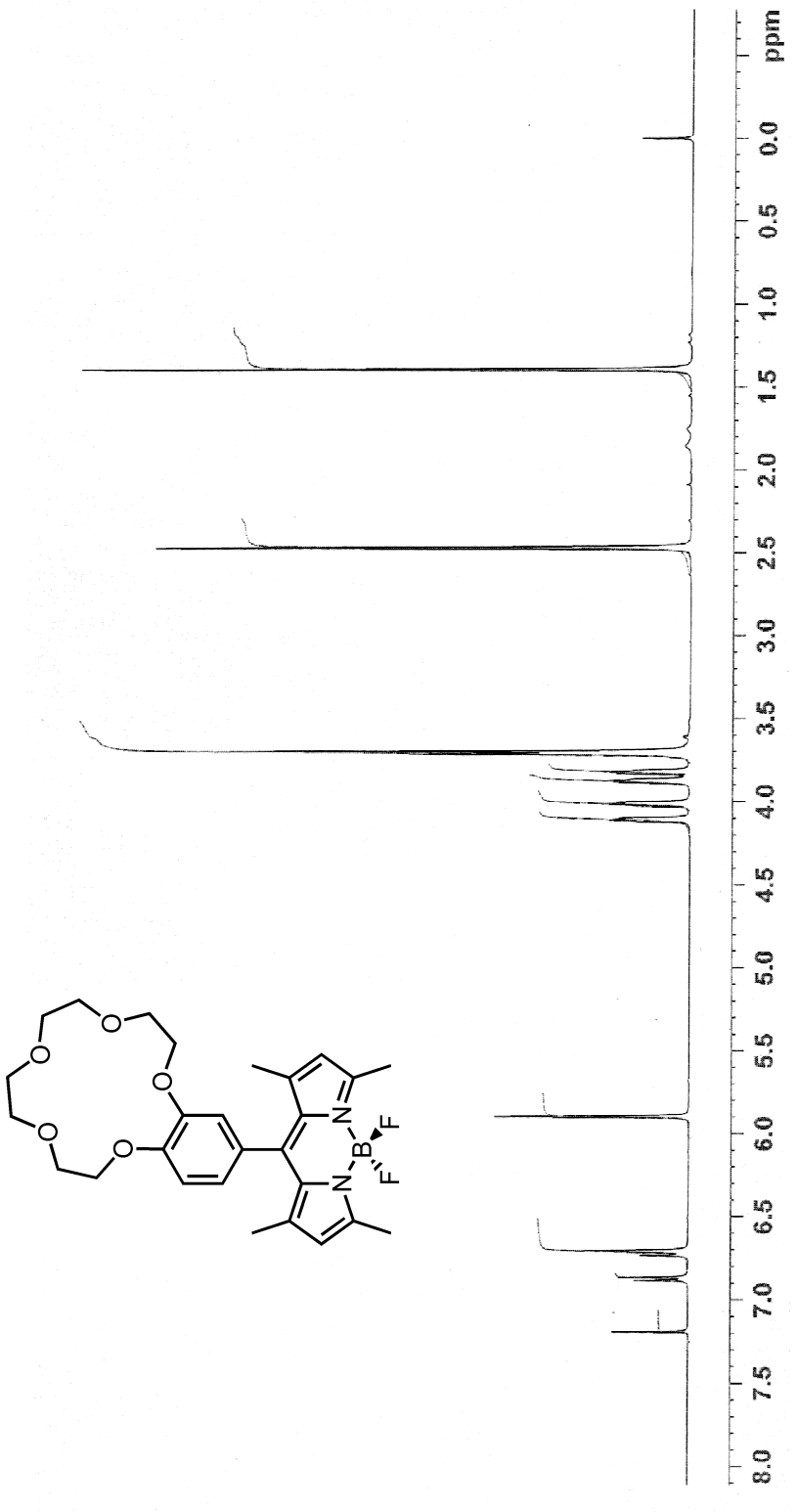

Figure 42 ^{1}H NMR Spectrum of compound **24**

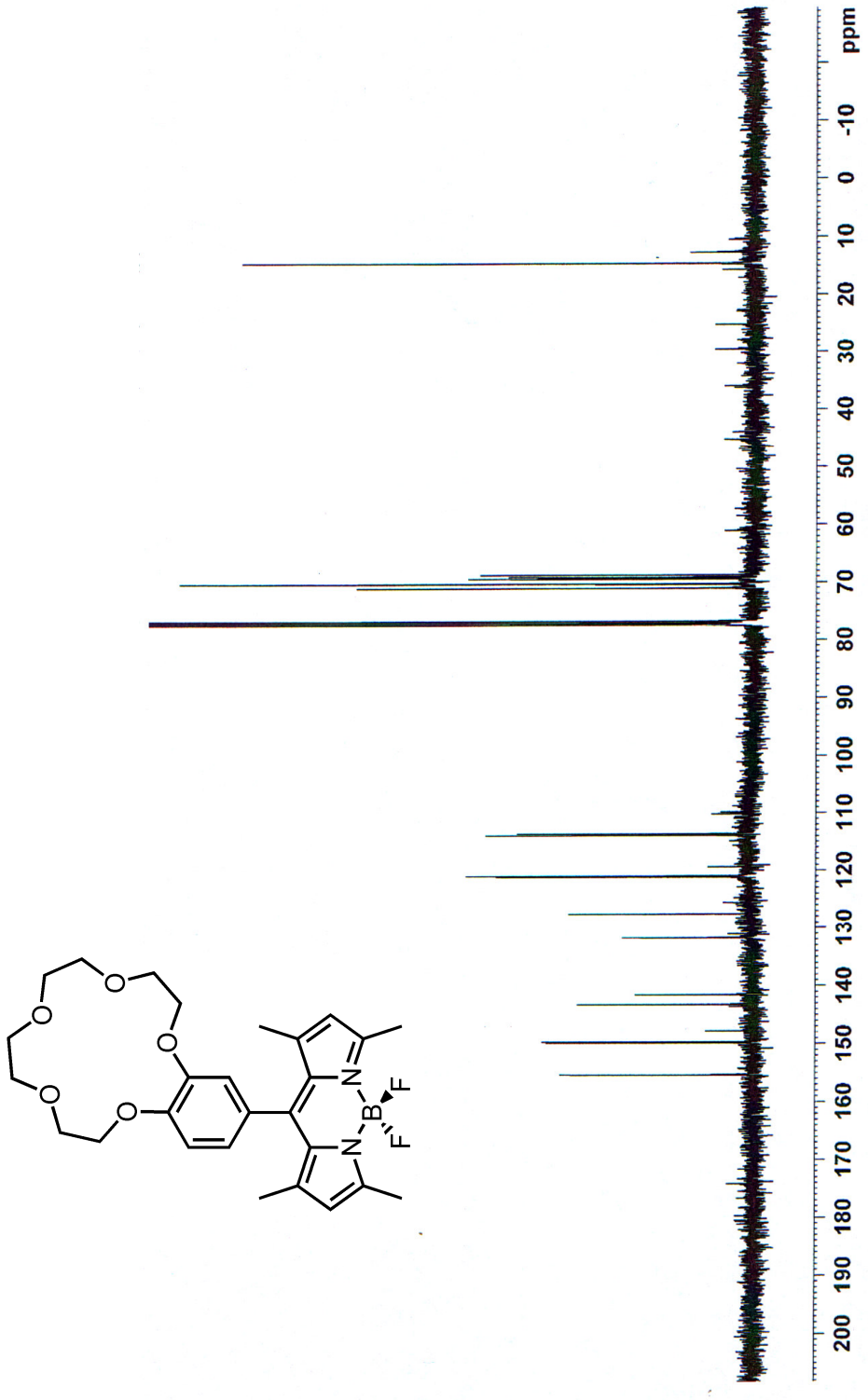

Figure 43 ^{13}C NMR Spectrum of compound **24**

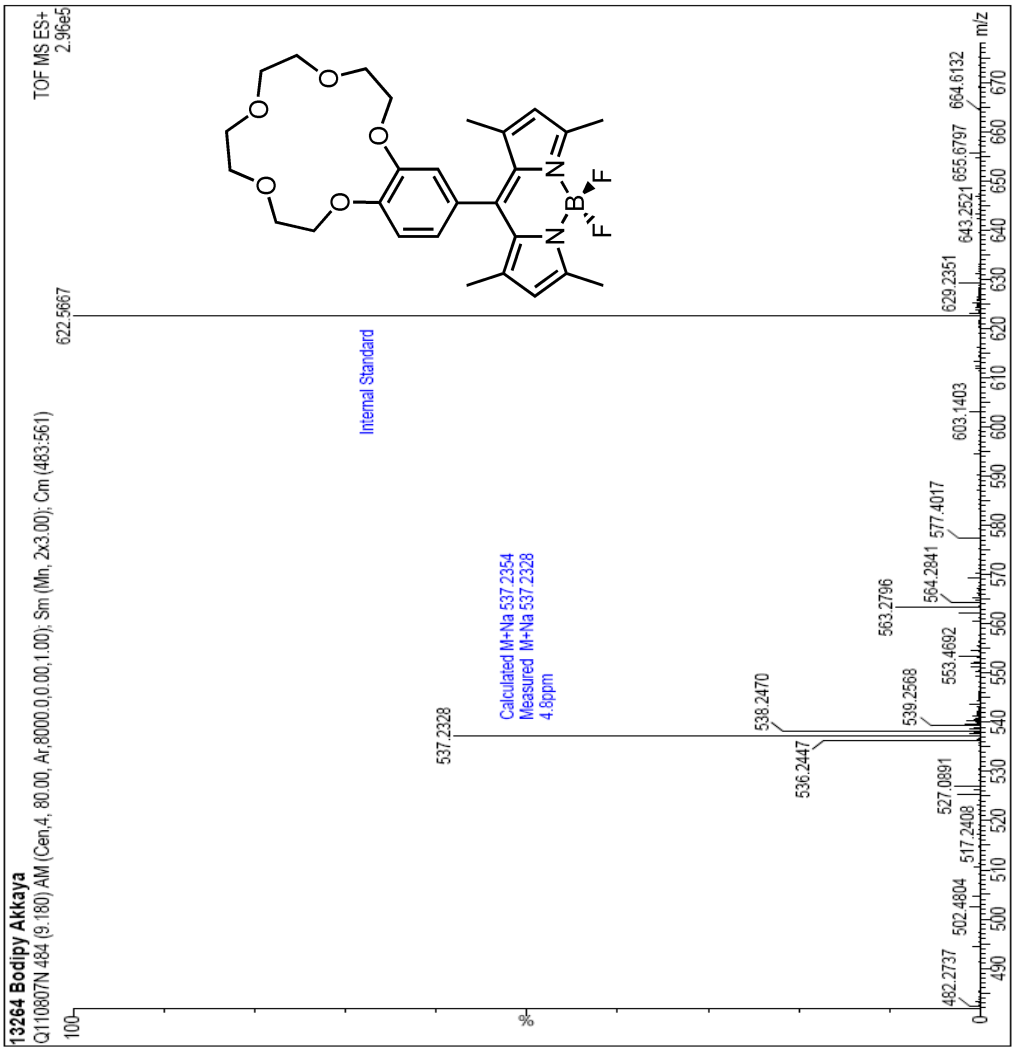

Figure 44 ESI-HRMS of compound **24**

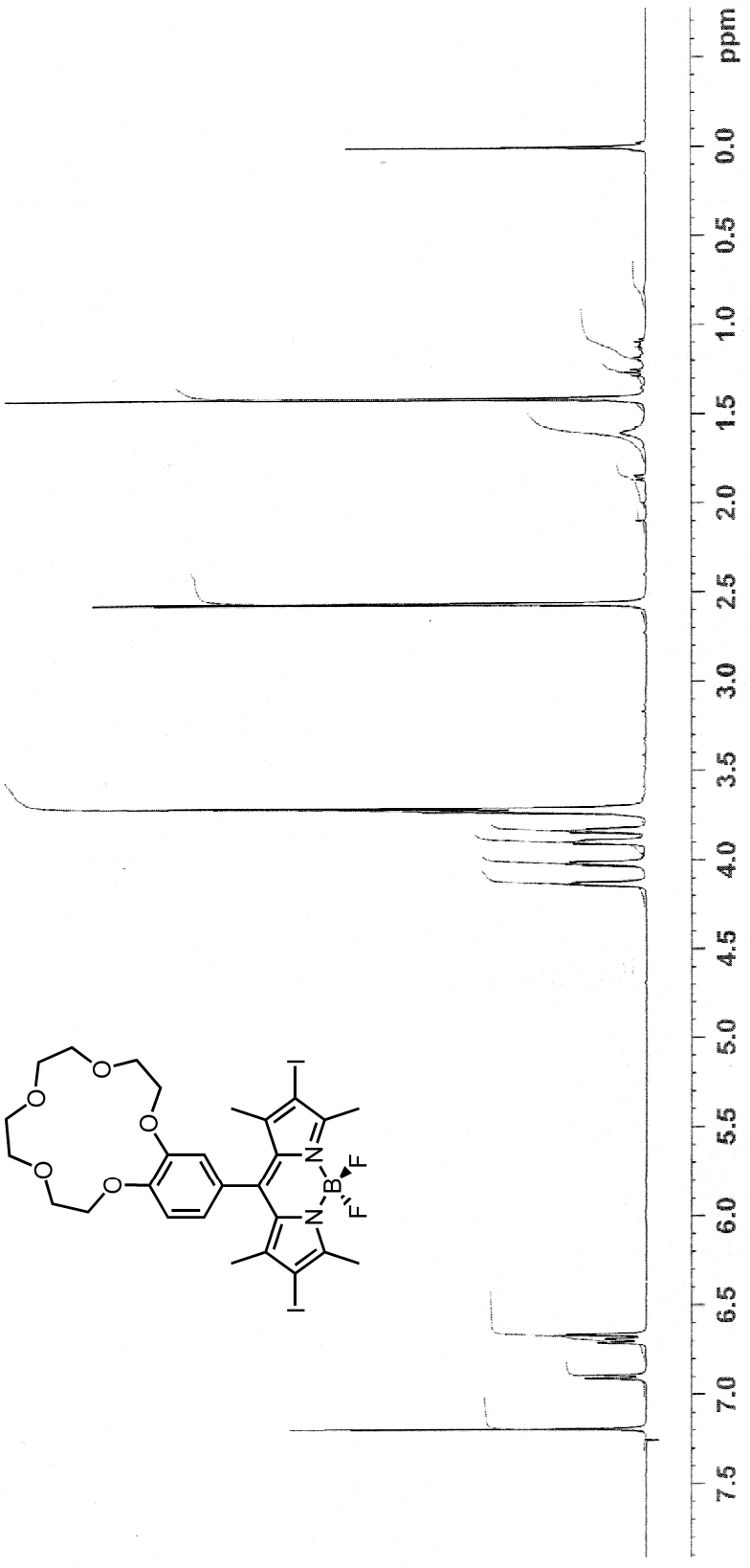

Figure 45 ^{1}H NMR Spectrum of compound **25**

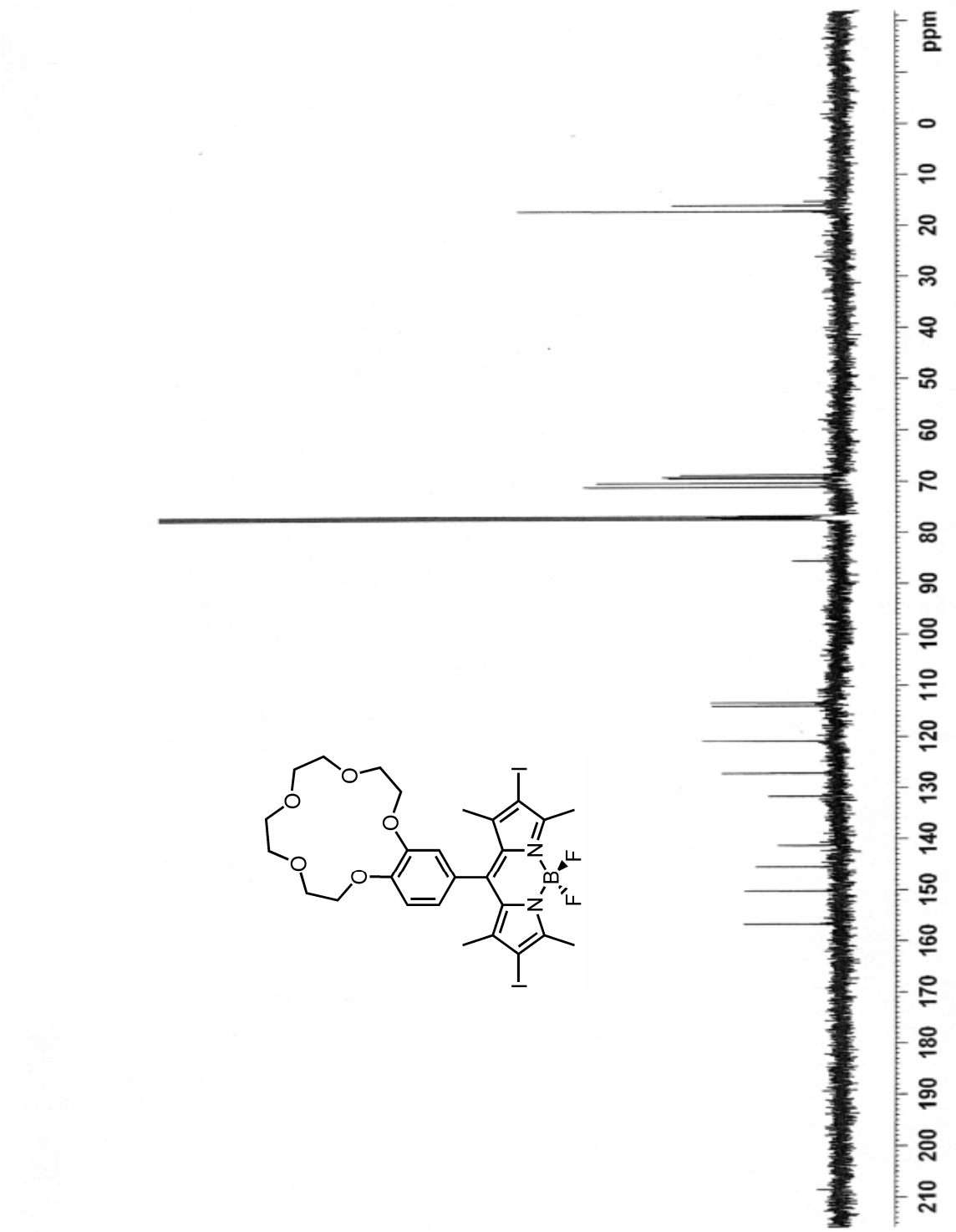

Figure 46 ^{13}C NMR Spectrum of compound **25**

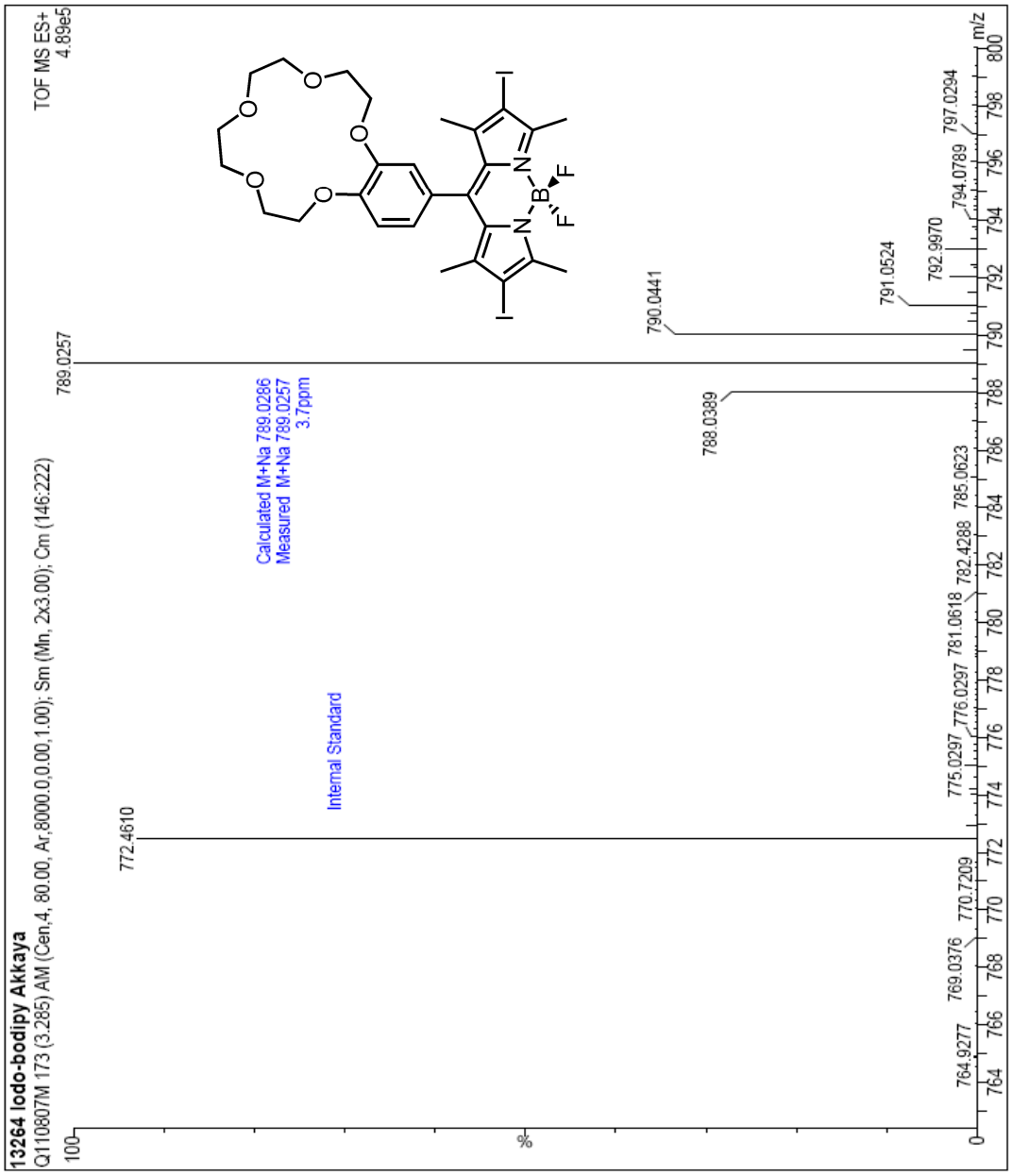

Figure 47 ESI-HRMS of compound **25**

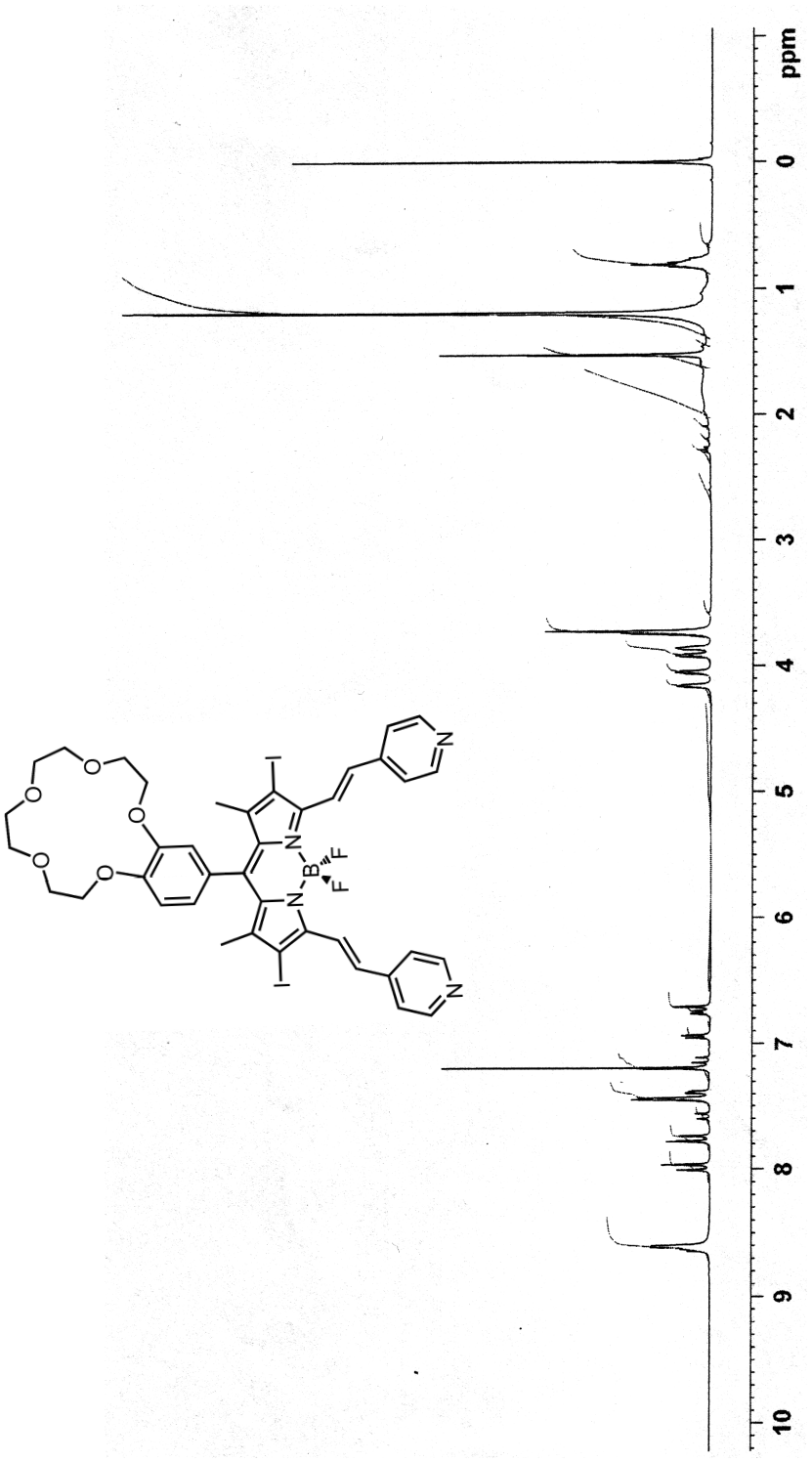

Figure 48 ^{1}H NMR Spectrum of compound **26**

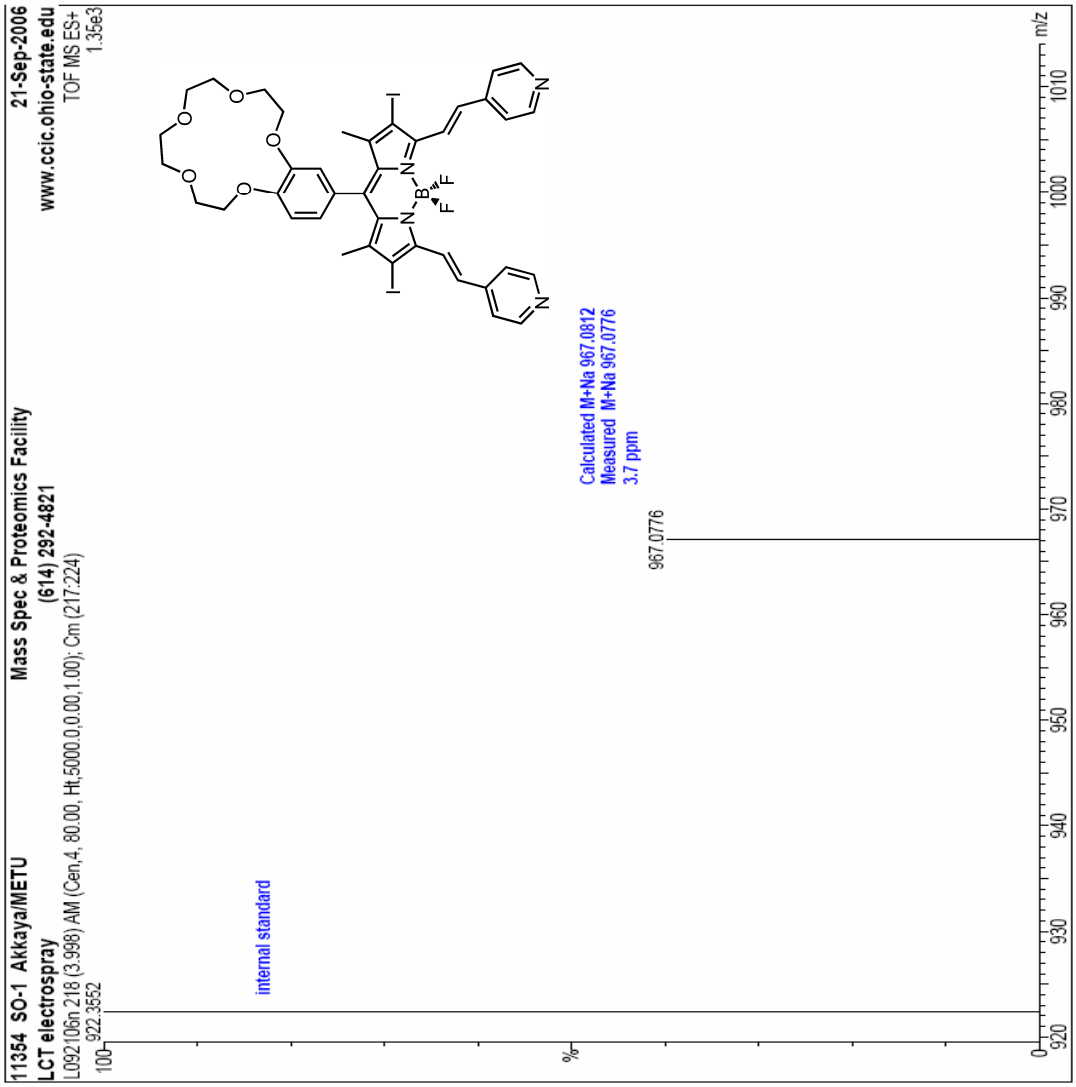

Figure 49 ESI-HRMS of compound **26**